Fall 2022

The Role of Actin Associated SPTBN1 Host Factor in HIV-1 Infection in Microglial Cells

Hannah Matheney
Missouri State University, Hannah023@live.missouristate.edu

THE ROLE OF ACTIN ASSOCIATED SPTBN1 HOST FACTOR IN HIV-1 INFECTION OF MICROGLIAL CELLS

A Master's Thesis

Presented to

The Graduate College of

Missouri State University

In Partial Fulfillment

Of the Requirements for the Degree

Master of Science, Cell and Molecular Biology

By

Hannah Matheney

December 2022

THE ROLE OF ACTIN ASSOCIATED SPTBN1 HOST FACTOR IN HIV-1 INFECTION IN MICROGLAL CELLS

Biomedical Sciences

Missouri State University, December 2022

Master of Science

Hannah Matheney

ABSTRACT

Human immunodeficiency virus (HIV) is a chronic illness affecting more than 32.7 million individuals worldwide. The virus infects immune cells, weakening the immune system overtime eventually leading to acquired immunodeficiency syndrome (AIDS) if left untreated. Infection starts with a fusion step, followed by uncoating of the HIV capsid once in the cytoplasm of the cell. HIV uses host cell proteins to complete the infection process, like the actin associated factor, SPTBN1. The Hulme lab has previously shown that SPTBN1 knockdown by siRNA in microglial cells decreased HIV infection and delayed uncoating of HIV. Because fusion is prior to uncoating, it is important to verify that fusion delay was not the reason uncoating was delayed. The goal of this thesis research was to further determine the role of SPTBN1 in HIV infection of microglial cells that are a natural host for HIV. The siRNA knockdown of SPTBN1 was optimized, achieving knockdown between 67-94%. A knockdown of SPTBN1 was done to confirm that it decreases infection, and the fusion kinetics were observed by a fusion assay. The fusion step of HIV infection was determined to not be affected by SPTBN1 knockdown with fusion kinetics being similar to control conditions. These results support the labs previous conclusion that SPTBN1 is involved in the uncoating step of HIV infection that follows fusion. Researching hosts factors such as SPTBN1 provide important insights to how HIV infects cells and identifies areas of interest that can be targeted by medications.

KEYWORDS: HIV-1, microglial, SPTBN1, cytoskeleton, actin

THE ROLE OF ACTIN ASSOCIATED SPTBN1 HOST FACTOR

IN HIV-1 INFECTION IN MICROGLAL CELLS

By

Hannah Matheney

A Master's Thesis
Submitted to the Graduate College
Of Missouri State University
In Partial Fulfillment of the Requirements
For the Degree of Master of Science, Cell and Molecular Biology

December 2022

Approved:

Amy Hulme, Ph.D., Thesis Committee Chair

Joshua Smith, Ph.D., Committee Member

Colette M. Witkowski, Ph.D., Committee Member

Julie Masterson, Ph.D., Dean of the Graduate College

ACKNOWLEDGEMENTS

I would like to thank the following people for their support during the course of my graduate studies. Those professors on my thesis committee, Dr. Joshua Smith and Dr. Colette Witkowski, thank you for taking the time to share your knowledge and advice as I was completing my thesis research. All of the past and present graduate students gave the best support as we are all in the same place. I am thankful for my family and friends supporting me and understanding the time requirements for completing a master's thesis. Most of all I want to thank Dr. Amy Hulme for being a tremendous advisor, being patient, knowledgeable, trusting, and all around showing me the excitement of research. I could not have completed this master's thesis to this standard without the huge amount of support.

TABLE OF CONTENTS

LIST OF TABLES

LIST OF FIGURES

INTRODUCTION

Human immunodeficiency virus (HIV) is the virus that causes acquired immunodeficiency syndrome (AIDS). From 1981 to 2019, 32.7 million people died from AIDS-related illnesses (1, 2). There are two types of HIV, HIV-1 and HIV-2. HIV-2 is less common in human infection, less pathogenic, and has a slower disease progression than HIV-1 (3). HIV is a virus that originated in monkeys as the simian immunodeficiency virus (SIV) that mutated to infect humans making it a zoonotic virus. The virus became infectious to humans in four cross species infection events where individuals came in contact with infected fluids. Each of these events led to a new group of HIV-1 virus (1, 4). The most common group of HIV-1 came from chimpanzees in Africa (1).

The four groups of the HIV-1 virus are M, N, O, and P. Determined based on the genetics of the viruses, the M and N groups were transferred to humans from the SIV of chimpanzees (4). The O and P groups are from SIV in gorillas (4). The M group of HIV-1 virus is the most common, accounting for 99% of the world's infections. Within the M group there are subtypes A, B, C, D, F, G, H, J, and K (4). The subtypes are created by the high mutation rate of HIV-1 due to the viral reverse transcriptase. The reverse transcriptase enzyme of HIV-1 has no proofreading activity, leading to a mutation rate of about 10^{-5} mutations per basepair for each replication cycle (4, 5). This mutation rate in the HIV RNA genome is much higher than mutation rates of 10^{-7} mutations per basepair within DNA viruses that do not use reverse transcriptase in the infection process (5, 6). There are also forms of the HIV-1 virus that are combinations of subtypes, called circulating recombinant forms (7). The high mutation rate makes it difficult to effectively target HIV-1 for treatment.

HIV is spread through infected blood, seminal fluids, breast milk, rectal fluids, and vaginal fluids (1). To establish infection, HIV-1 targets immune cells with CD4 receptors present on their membrane (8, 9). These cells help fight bacteria and viruses that enter the body, so it is important to have many healthy CD4+ cells. A normal CD4 cell count is between 500 to 1500 cells per millimeter^3 of blood. The HIV-1 genome integrates into the CD4+ host cell genome and activates the DNA damage response. The activation of DNA-dependent protein kinase causes a signal cascade that causes the death of the CD4+ cells after the HIV-1 infection process (10). HIV-1 infection causes the decreased CD4 count of patients as the disease progresses. This prevents the immune system from being able to properly fight off infections within the body (11).

HIV-1 infection proceeds through three clinical phases. The first stage is acute HIV-1 infection, where the individual is highly contagious due to large amounts of HIV-1 in their blood and is characterized by mild flu-like symptoms (1, 2). This first stage happens a couple weeks to a month after HIV-1 infection and can last a few days to weeks with a wide range of symptoms. The second stage of HIV-1 progression is the clinical latency or chronic HIV-1 infection. The viral load is very low in the body and individuals usually have few if any symptoms of infection. This stage, without treatment, can last 10 to 15 years for regularly progressing individuals with a gradual decrease of CD4+ cells as time goes on (1, 2). During this stage, HIV-1 has inserted its genome into host cells but is not being replicated, creating the viral reservoir and latent infection (1). The last stage of HIV-1 infection is the progression to AIDS. AIDS is due to the body's immune system being weakened by the virus, allowing for opportunistic infections to occur. Individuals are diagnosed with AIDS when their CD4 count is less than 200 cells per millimeter^3 of blood, down from the 500 to 1500 normal cell count, or an individual develops opportunistic

infections (1, 2). During the last stage of HIV-1 progression, individuals have high viral loads and are very infectious (1, 2). The life expectancy of someone with AIDS without treatment is approximately a year, where death is a result of infections from the weakened immune system.

LITERATURE REVIEW

HIV-1 and the Immune System

Target cells of HIV-1 includes dendritic cells, CD4+ T cells, and macrophages (8, 12). These cells are all part of the human body's immune system responsible for recognizing foreign harmful molecules in the body and fighting them off. It is a complex network of cells signaling one another to initiate a response to a potential harm (13). The immune system has two parts: the innate immune system and the adaptive immune system. The generalized immune response is the innate immune system that works quickly when a foreign molecule first tries to enter the body. The innate immune system relies heavily on membranes of the body to physically prevent germs from entering. If the foreign molecule enters the body, many immune cells go toward the site of entry to destroy the molecule. The cells involved in this response includes granulocytes, mast cells, macrophages, and dendritic cells (14–16).

The adaptive immune system is a specialized response to foreign molecules in the body. The adaptive immune response activates if the innate immune response fails to fight off the foreign molecule that entered the body. This is a slower response because the cells must specifically identify the pathogen to fight it. Though this is a slower response, it is more long term because the cells recall a pathogen if it has fought it off once. If the foreign molecule enters the body again, the adaptive immune system will quickly and effectively fight off the infection. The cells involved in the adaptive immune system include B cells and T cells (15, 16) . These cells will increase the immune response by signaling and recruiting other immune cells to the area of infection.

The HIV target cells are important for the immune system to work properly. Macrophages are derived from monocytes as part of the innate immune response. Macrophages

engulf bacteria to destroy them. Dendritic cells are antigen-presenting cells involved in the innate immune system that can also be derived from monocytes. Dendritic cells receive the antigens from their environment and recognize pathogens. The antigen presented on the cell is recognized by adaptive immune cells to specifically target pathogens. B cells and T cells as part of the adaptive immune system will bind to the antigen presented on the dendritic cell and use it to ramp up the immune response (16). T cells will recruit other immune cells to better fight and destroy the pathogen. The immune system and all cells involved are required to keep us healthy. HIV infection disrupts the ability of the immune system to properly fight off infection because it infects the immune cells themselves.

Different immune cells are specialized and localized to various areas of the body to be the most effective at fighting off illness at those areas. Microglial cells are specialized macrophages present in the Central Nervous System (CNS) at high quantities and a natural host for HIV-1 (17). Microglial cells are primarily responsible for the innate immune system within the CNS. These immune cells are slow growing and can survive for over four years. Microglial cells are the long-lasting cells when infected with HIV-1 and cause incessant infection that prevents eradication (17). These cells contribute to the viral reservoir with HIV-1 permanently integrated into their genome, leading to the progression of the disease (17). The viral reservoir is the biggest barrier for curing HIV infection.

Microglial cells are the largest part of the HIV viral reservoir in the brain. The viral DNA lays dormant in the cell and with every division cycle the new cells contain the HIV genome as well. The microglial cells can then be activated through various extracellular factors including different cytokines and chemokines. Increase of the viral loads further progresses patient illness during the end of the chronic HIV infection stage (18). It is biologically relevant to study these

natural host cells that make up the HIV reservoir. The microglial cells are especially important when talking about HIV-1 associated neurocognitive diseases (HAND). When HIV-1 infects microglial cells, it can cause them to release neurotoxic factors and cause neuron degeneration. These natural host cells are important to study and understand for treating HIV-1 and HANDs it can cause.

Treatments for HIV-1 Infection

There is currently no cure for HIV-1 infection, but since the epidemic began there has been great progress in treatments for infected individuals as well as preventative treatments for high-risk groups. Individuals more likely to encounter HIV-1 contaminated fluids are within these high-risk groups. High-risk individuals can work to prevent HIV-1 infection by avoiding using nonsterile syringes, using protection during sex, and taking preventative prescription therapies. For individuals at increased risk of HIV-1 infection there is pre-exposure prophylaxis (PrEP) medication available (1). Anyone that has recently been exposed to HIV-1 may take post-exposure prophylaxis (PEP) medications to prevent infection. After someone has been infected and is HIV-1 positive, there are also medications to prevent the progression of the disease. These medications, called antiretroviral therapies (ART), work to reduce the HIV-1 viral load in the body, slowing the progression of the disease and helping to prevent new infections (1). For these therapies to be effective, they must be taken consistently as prescribed to keep the viral load low.

Antiretroviral therapy is a lifelong treatment to prevent HIV-1 infection progression. Individuals should start ART as soon as possible after HIV-1 infection to slow progression of symptoms (1, 7, 19). The types of ARTs disrupt specific HIV-1 replication processes including nucleotide reverse transcriptase inhibitors (NRTI), non-nucleoside reverse transcriptase

inhibitors (NNRTI), integrase inhibitors (INSTI), protease inhibitors (PI), entry inhibitors, or a combination thereof (7, 20).

Each of these have a slightly different mechanism to block HIV-1 infection. NRTIs are structured similar to a nucleotide that would be added during the reverse transcription process but does not have a 3' hydroxyl for the next base of DNA to add on to. This drug treatment halts reverse transcription, stopping the HIV-1 infection process (20). NNTRIs also work to stop reverse transcriptase activity, but these bind to the enzyme creating a hydrophobic site near the active site that prevents efficient reverse transcription. The reverse transcription activity is greatly decreased and helps prevent further HIV-1 infection (20). INSTIs block the transfer of the viral DNA into the host cell genome by binding to the integrase active site. Integration of the viral DNA into the host cell genome is required for subsequent HIV-1 infection (20). PIs act in a similar way to INSTIs by binding to the enzyme, in this case protease, and preventing it from performing its function. The protease enzyme is involved in the maturation of HIV-1 virus by cleaving the polyproteins into separate proteins. The cleavage of the proteins is needed for the virus to mature and be able to infect further cells (20). The final treatment option is a multitude of entry inhibitors. These work to prevent HIV-1 from enter any host cells, stopping the infection process before it starts (20).

Treatment plans often include multiple types of medications used in combination. This combination therapy works at multiple steps in the HIV-1 replication process to help prevent progression of the disease (7). Due to the high mutation rate of HIV-1, resistance to the medications occurs easily if the patient is not adhering to their treatment plan (7). The HIV-1 replication cycle and structure are researched widely to find more effective treatments for patients.

Structure of HIV-1

An HIV-1 virion is an enveloped virus particle that includes the RNA genome surrounded by a protein capsid. The structure of HIV-1 contains two RNA copies of the viral genome to encode the three polyproteins and various accessory proteins (21). The three polyproteins are the group-specific antigen (Gag) protein, the polymerase (Pol) protein, and the envelope glycoprotein (Env; ((21)). Each of the polyproteins is cleaved into multiple separate proteins. The Gag protein is cleaved by a viral protease to form the matrix (MA), capsid (CA), and nucleocapsid (NC) proteins. The Pol is cleaved by a viral protease to form the enzymes of the virus; protease (PR), reverse transcriptase (RT), and integrase (IN; (21)). The Env polyprotein is what makes up the envelope of the HIV-1 virus which includes the surface (SU) Env glycoprotein, gp120, and the transmembrane (TM) glycoprotein, gp41 (21). The Env polyprotein is cleaved by a host cell protease, unlike the viral protease that cleaves the Gag and Pol proteins (21). The Pol, Env, and Gag proteins are essential in the replication process of HIV-1.

A few regulatory and accessory proteins are encoded by the HIV-1 genome as well. The trans-activator of transcription protein (Tat) plays a role in transcribing the HIV-1 genome (21). The Tat protein activates the transcription of the viral long terminal repeat (LTR) promoter (22). The 5' LTR contains the promoter for the viral genes integrated into the host cell (22, 23). Transport of the viral RNA from the nucleus to the cytoplasm requires the RNA splicing-regulator (Rev) protein encoded within the HIV-1 genome (21). The Rev protein has a nuclear localization signal and RNA binding sites to export viral RNA from the nucleus for translation to occur in the cytoplasm (24).

The accessory proteins present in the structure of HIV-1 are Nef, Vpr, Vpu, and Vif (21, 23). The negative factor (Nef) is involved in the downregulation of the CD4 receptor and major histocompatibility complex I, as well as the activation of p21-activated protein kinase to improve the ability of a virion to infect a cell (25). The viral protein R (Vpr) has many roles in increasing infectivity of the HIV-1 virus, especially in macrophages. Vpr increases replication of the virus, increases the effect on T cells, and is one of the most prevalent proteins within the HIV-1 virion (26). The viral protein U (Vpu) is a viroporin that can modify membranes to help with trafficking in the cell and release of HIV-1 from the host cell (23). Vpu is also involved in the downregulation of CD4 receptors on the host cell (27). The viral infectivity factor (Vif) plays a major role in ensuring infection of the virus. Vif binds to the immune factor APOBEC3G, that usually targets and destroys retroviruses, to instead initiate the ubiquitination and degradation of APOBEC3G, allowing for the survival of HIV-1 (28). APOBEC3G, encoded by HIV-1 host cells, is a DNA editing enzyme that has antiviral properties making it a restriction factor (29). Vif is an important viral factor for efficient HIV-1 infection, protecting against the antiviral effects of APOBEC3G (29).

The structure of the HIV-1 virion is vital for the efficient infection of a host cell (Fig. 1). The arrangement of the proteins within the mature virus starts on the membrane with the Env proteins gp120 and gp41. The gp120 protein (pink in Fig. 1) is on the outside of the virus and binds to the host cell membrane proteins. The gp41 protein is the transmembrane protein (green in Fig. 1) that attaches the gp120 protein to the membrane of the virus (30). Both gp41 and gp120 proteins are involved in the fusing of viral and host cell membranes (23). The matrix protein localizes just under the membrane of the HIV-1 virus (light blue in Fig. 1). The capsid proteins form a conical structure surrounding the viral genome (dark blue in Fig. 1). The HIV-1

capsid is made of approximately 1,500 capsid monomers that form hexamers and a few pentamers to make the conical structure (31). The viral RNA within the capsid has nucleocapsid bound to it, protecting it and forming the RNA complex (black RNA with yellow NC in Fig. 1; (23, 30, 32)). The reverse transcriptase (orange in Fig. 1) and integrase enzymes are held within the capsid core enabling them to interact with the viral RNA (30). The reverse transcriptase enzyme converts the viral RNA to DNA that is processed at the LTR regions by integrase that also incorporates the viral DNA into the host cell DNA (23).

HIV-1 Replication Cycle

Binding of the virus to a host cell receptor is the start of the replication cycle for HIV-1 allowing for fusion of the host and viral membranes (Fig. 2 step 1; (9, 33)). The HIV-1 envelope protein gp120 binds to the CD4 receptor on target cells (9). When the virus binds to the CD4 receptor on a host cell, a conformational change occurs allowing a bridging sheet domain to form. The new domain becomes the binding site for the co-receptor, either CCR5 or CXCR4. The CCR5 co-receptor is the most common and helps stabilize the membrane proteins once bound to the CD4 receptor (9). The gp41 protein attached to the gp120 protein in the envelope of HIV-1 has a conserved sequence called a fusion peptide that initiates fusion of the two membranes (33). After receptor binding, the fusion peptide inserts itself into the host cell membrane. The gp41 protein then forms a stable trimeric 6-helix bundle that brings together the two membranes for fusion (33).

Once the viral membrane and host membrane fuse, the HIV-1 viral core is released into the host cell cytoplasm where uncoating and reverse transcription initiate to turn the viral RNA into DNA (Fig. 2 step 2 and 3; (31, 34, 35)). Reverse transcription is carried out by reverse transcriptase starting at the 3’ C terminal end of the viral RNA converting it into double stranded

DNA and creating the reverse transcription complex (RTC; (35)). This complex contains viral RNA, newly made DNA, and various associated viral proteins including CA (36). Reverse transcription initiates in the cytoplasm and is completed once in the nucleus (31, 37). Research has shown that some intact capsid must be associated with the RTC when the viral genome enters the nucleus as it interacts with the nuclear pore (31, 34). The RTC forms into the pre-integration complex (PIC) once the viral RNA is completely converted into DNA (Fig 2. Step 4; (31, 37)). The reverse transcribed viral DNA contains long-terminal repeats on the ends that are processed by integrase, preparing the viral DNA for integration into the host cell genome (38, 39). The integrase binds to the LTR and carries out endonuclease cleavage to remove two nucleotides that allow for the strand transfer process to begin. The strand transfer integrates the viral DNA into the host cell DNA (40). The order of HIV-1 infection steps uncoating, reverse transcription, and nuclear import are not entirely known as each step may have different mechanisms depending on the host cell. Uncoating is the process of the HIV-1 viral capsid core subunits disassociating from the reverse transcription complex (RTC; (31)).

Given these data, there are three main models of HIV-1 uncoating and reverse transcription including the cytoplasmic, nuclear pore complex (NPC), and nuclear uncoating models (Fig. 3). A previous model that has been widely disproven is the immediate uncoating model (41–43). This model proposed the HIV-1 capsid disassociated from the genome almost immediately after fusion with the host cell (31). The three current models are representations of ways reverse transcription and uncoating may occur during HIV-1 infection, with evidence supporting all three (31, 42). The cytoplasmic uncoating model has the capsid slowly disassociating as it moves toward the nucleus of the cell and reverse transcription happening at the same time (Fig. 3 left). The NPC uncoating model describes the capsid remaining stable until

it docks at the nuclear pore where the reverse transcribed viral DNA enters the nucleus (Fig. 3 middle; (31)). The newest model of capsid uncoating is the nuclear model. This model has the entire HIV-1 capsid entering the nucleus of the cell before uncoating occurs (Fig. 3 right; (42)). The process of uncoating is uncertain but likely to occur as one of these models or a combination thereof depending on the host cell.

Research has shown various results about where reverse transcription and uncoating start and finish. Reverse transcription most likely starts in the cytoplasm and finishes within the nucleus (37). There are reverse transcription molecules shown within the nucleus. Uncoating of the capsid may start in the cytoplasm or occur at docking and import into the nucleus (36, 37, 43). Capsid molecules have been shown to be associated with the HIV genome while in the nucleus, but it is not known the extent or configuration of the capsid remaining intact when in the nucleus (44). The mechanisms of uncoating may also depend on the cell that is being infected as different host factors can affect the infection process.

The previous steps of replication, binding, fusion, reverse transcription, and uncoating, are happening at the host cell membrane, in the cytoplasm, and finishing in the nucleus of the cell (Fig. 2 and 3). The HIV-1 complex enters the nucleus through a nuclear pore complex (NPC). NPCs are embedded in the membrane of the nucleus of the host cell and regulate movement in and out of the nucleus. The NPC is made of nucleoporins (Nup) that interact with molecules such as the HIV-1 genome. The viral DNA is trafficked to the NPC where nucleoporins assist in the nuclear import process (Fig. 2 and 3; (45)). The proper translocation of HIV-1 through the NPC is thought to specifically rely on Nup153 and Nup358. Nup358 forms a basket on the cytoplasmic side of the NPC while Nup153 forms a similar structure on the nucleoplasm side (46). Once the HIV-1 DNA is in the nucleus, the integrase on the ends of the

DNA catalyzes the integration of the viral DNA into the host genome (Fig. 2 step 4; (47)). The stages of HIV-1 replication up to integration are considered the early stages of infection.

After integration of the HIV-1 genome into the host cell genome, HIV-1 starts to replicate within the host. The HIV-1 genome is transcribed within the host cell and using the cells machinery. The HIV-1 RNAs are exported out of the nucleus and are translated to the polyproteins: Gag, Pol, and Env (Fig. 2 step 5; (48)). These polyproteins localize to the surface of the host cell membrane. With all HIV-1 proteins at the host cell membrane, the virus buds off (Fig. 2 steps 5 and 6). After the HIV-1 virus buds from the host cell the virus cleaves the polyproteins and organizes them creating the mature HIV-1 virus that can infect other cells (Fig. 2 step 7; (48)).

Cytoskeletal Function in HIV-1 Infection

The infection process of HIV-1 is assisted by cellular host factors. These factors contribution to infection can be observed through knockdowns of the protein factors and observing the effect on HIV-1 infection. Oppositely, HIV-1 restriction factors are within the host cell and prevent effective infection, like the previously mentioned APOBEC3G. When APOBEC3G is present, there is a lower HIV-1 infection efficiency (49). Inhibition of cytoskeletal factors like Rho GTPase, cause a decrease in HIV-1 infection (50). Rho GTPases are involved in actin organization specifically, but many factors associated with both actin and microtubules are known to play a role in HIV-1 infection (50).

During infection the viral complex is trafficked through the cytoplasm towards the nucleus with the help of host cell microtubules (51–54). Microtubules are dynamic structures in all cells made of tubulin molecules. Microtubules have many responsibilities in the cell including providing shape and trafficking throughout the cell by the motor proteins kinesin and dynein.

The motor proteins can associate with many factors that regulate processes within the cell. Both proteins can carry cargo along microtubules with dynein moving towards the nucleus and kinesin moving towards the periphery of the cell (54). The HIV-1 capsid core interacts with the microtubule cytoskeleton to assist in uncoating, reverse transcribing the viral RNA, and migrating toward the nucleus (51–53). The polar movement of the motor proteins could play a role in HIV-1 uncoating, by pulling apart the capsid structure (31, 52). A knockdown of microtubules within the host cell delays capsid uncoating. There are a few models suggesting how uncoating occurs, but the exact process is not known (31). The HIV-1 capsid interacts with microtubules but the capsid interaction with other cytoskeletal elements, such as actin, is also being studied.

Though research has shown that HIV interacts more with microtubules, it also associates with actin filaments. Microtubules are used more in long distance trafficking of HIV towards the nucleus while actin trafficking is shorter distances (54). The microtubules generally are important for cell division, creating intracellular pathways during interphase where the microtubule motor proteins carryout mitotic processes. Microtubules are essential for metaphase as they organize the chromosomes and pull apart the sister chromatid to ensure each daughter has the same number of chromosomes (55). When HIV-1 infects a cell, it recruits microtubule associated proteins that stabilize the microtubules and allow for trafficking to the nucleus (6). The actin cytoskeleton is highly involved in cell communications, cell to cell signaling, and movement of cells. Actin polymerization also occurs during phagocytosis and endocytosis at the location to change the cell structure and plasma membrane to envelope the molecule (55). Actin polymerization allows for cells to be motile with many of the processes requiring the myosin motor protein.

Actin knockdown has also shown a negative effect on HIV-1 infection (54, 56). Actin is found in all eukaryotic cells at a high abundance. It consists of globular subunits that arrange in a line to create the filamentous F-actin structure that creates actin bundles and networks (57). The F-actin is linked by proteins that help form the essential actin structure. The network of actin is highly involved in the structure of the cell, located just under the plasma membrane. Actin organization within the cell allows the cell to keep its shape and participates in various cellular processes such as trafficking of material (57). Actin organizing factors are important in polymerization and function of the cytoskeleton. Actin may play a role in the cytoplasmic stages of HIV-1 infection with the most prominent involvement in viral entry and budding, as those are processes directly involve the plasma membrane.

The CD4 receptor and co-receptors are brought together on the host cell membranes by actin (58). The binding of HIV-1 to the CD4 receptor on the host cell receptor causes polymerization of actin at the binding location (59–61). Viral budding from the host cell membrane or through a cell to cell transfer has high actin colocalization as well (58, 62, 63). The actin motor protein, myosin, may move the HIV-1 complex within the host cell, though to a lesser extent than the microtubule motor proteins (54, 64). Closer to the nucleus, smaller movement of the viral complex occurs that is likely due to actin. Actin movement of viral particles is smaller and may be an intermediate step before the virion is transferred to microtubules (6, 59). During assembly and budding of virus, actin has been shown to help viral proteins assemble at the host cell membrane (58). It is likely that actin is involved in more of the HIV-1 infection stages (65). The network of the actin cytoskeleton is necessary for the survival of the cell, but what exact role the associated proteins play in HIV-1 infection could provide insight to the timeline of infection and replication within the host cell.

SPTBN1 and HIV Infection

Proper actin polymerization within the cell is essential for efficient HIV-1 infectivity (66, 67). This thesis research focuses on the actin cytoskeletal element spectrin beta nonerythrocytic 1 (SPTBN1; (56)). SPTBN1 is a cellular factor associated with host cell membranes and the actin cytoskeleton (68). SPTBN1 encodes for a filamentous beta-spectrin molecule that is found in nonerythrocytic cells (69). Spectrin family proteins provide support and shape to cells by interacting with the actin cytoskeleton as a scaffolding protein (56). Scaffolding proteins interact with and organize different molecules, in this case actin. Spectrin molecules are polymers of alpha (Fig. 4A brown) and beta spectrin (Fig. 4A yellow) molecules. The structure contains at least 20 alpha spectrin repeats connected to at least 16 beta spectrin repeats to form a heterodimer. This strand creates a tetramer with another heterodimer strand that aligns antiparallel (68, 70, 71). Beta spectrin molecules have an N-terminal actin binding domain (Fig. 4A pink) and a varying C-terminal domain (Fig. 4A; (71)). The spectrin helices are connected by a linker series (Fig. 4B). The helical structure allows the spectrin molecules to grow and shrink based on what is necessary for the cell at the time (71).

The interaction of SPTBN1 with other host factors facilitates organization of the actin network within the cell (72). A study by Brass in 2009 indicated that SPTBN1 is an HIV-dependency factor or a protein required for HIV-1 replication that is expressed in the host cell (68). The same study showed that knockdown of the SPTBN1 protein decreased the ability of pseudotyped vesicular stomatitis virus G (VSV-g) HIV to infect HeLa cells (68). A pesudotyped virus is made in the lab with a separate plasmid expressing a different envelope and a deletion of the envelope gene from the viral genome. A common envelope used is the VSV-g protein envelope. This pseudotyping prevents the HIV virus from infecting more than one cell due to the

HIV envelope not being expressed, ensuring safety in the lab. VSV-g pseudotyped HIV has a different mode of entry into the host cell, by endosome fusion rather than at the membrane. Endosome fusion is where the HIV-1 virion enters the cell through an endosome that requires acidification of the endosome to release the capsid into the cytoplasm of the host cell (73). The involvement of HIV-1 with cytoskeletal elements and the indication that SPTBN1 alterations affects HIV-1 infectivity, indicates the factor is involved in the HIV-1 replication process (56, 68, 74).

Another study by Gallo tested the infectivity variation with different viral envelope proteins present, after SPTBN1 knockdown (74). The Gallo study did a knockdown of various HIV-1 dependency factors involved in viral trafficking towards the nucleus, including SPTBN1, and infected HeLa cells with wildtype or pseudotyped HIV-1 virus. The factors all decreased HIV-1 infection with the wildtype envelope but only knockdown of Dynein Axonemal-Light Chain 1 (DNAL1) and Microtubule Associated Protein 4 (MAP4) had the same decrease of infection with the pseudotyped HIV-1 virus and were the main focuses of the study after that. For the purposes of this thesis it is important to note that the Gallo study in HeLa cells showed that siRNA knockdown of SPTBN1 did not decease infection of VSV-g pseudotyped HIV as significantly as wildtype enveloped virus (74). This conclusion disagreed with a later study in the Dai lab that had the same decrease of HIV infectivity in macrophages with wildtype or pseudotyped virus (56, 74).

Further research has shown that SPTBN1 is a host factor that enhances HIV-1 infection. Suppressing SPTBN1 decreased HIV-1 infection in macrophages (56). The research by Dai focused on interleukin 27 (IL-27) as the inhibitor of SPTBN1 and a possible therapeutic treatment for HIV-1 infection. IL-27 activates differentiation of monocytes into macrophages.

Macrophages induced by IL-27 suppress SPTBN1 production and resist HIV-1 infection. Macrophages that do not express IL-27 are susceptible to HIV-1 and HIV pseudotyped virus infection (56). This research further supported the theory that SPTBN1 is required for HIV-1 infection of macrophages and may be an enhancing factor for infection in other primary cells. SPTBN1 may work to enhance infection after fusion with the host cell and before reverse transcription of the viral RNA is complete as it interacts with the matrix and capsid proteins (56). The knockdown of SPTBN1 greatly disrupted the actin cytoskeleton and decreased HIV-1 infection (56). The role of SPTBN1 and HIV-1 protein interaction at early stages of HIV infection may give a better idea of what is happening at those times.

Previous Research

Based on three previous studies, the Brass, Gallo, and Dai works, the cellular factor SPTBN1 is involved in HIV-1 infectivity. Marc Havlicek, a previous graduate student in Dr. Amy Hulme's lab, showed that 38.7% knockdown of SPTBN1 decreased infectivity of HIV-1 by 37.58%. The SPTBN1 knockdown of 38.7% was the highest achieved. Marc Havlicek also found that knockdown of SPTBN1 delayed uncoating in microglial cells by performing a CsA washout assay. This indicates that SPTBN1 is involved in the uncoating step of HIV infectivity (75).

Aims and Hypotheses

This research will continue the research of Marc Havlicek to verify the effect of SPTBN1 knockdown on HIV-1 infectivity, examine the effect of SPTBN1 on viral fusion, and the association of HIV-1 virions with the actin cytoskeleton after SPTBN1 knockdown. The first aim of this research is to optimize the siRNA knockdown protocol of SPTBN1 and investigate the effect on HIV-1 infectivity in microglial cells. Microglial cells are used because they are natural

hosts for HIV-1 and are part of the viral reservoir that prevents curing HIV-1 infection. Initial siRNA knockdown and qRT-PCR protocols will be enhanced through comparison of multiple siRNA knockdown protocols and qRT-PCR reagent systems. After the optimized SPTBN1 knockdown procedure, the CHME3 microglial cell line will be infected with VSV-g pseudotyped HIV-1 GFP reporter virus. The GFP reporter is added into the HIV-1 genome and expressed when the virus infects a cell. The GFP expression represents the infectivity of the VSV-g-GFP HIV virus. Infectivity of the virus will be calculated through flow cytometry to quantify infected cells by GFP expression. The knockdown cells will be compared to a non-targeting siRNA control. The microglial cells transfected with siRNA to knockdown SPTBN1 will be harvested for RNA. The isolated RNA will be used for qRT-PCR to confirm the fold-decrease of SPTBN1 knockdown.

It is hypothesized that the down regulation of SPTBN1 in microglial cells will decrease infectivity of HIV-1. Down regulation of SPTBN1 is shown in the Dai study to decrease infectivity of HIV-1 within macrophages, as well as briefly discussed in the Brass and Gallo on HeLa cells. Marc Havlicek's research showed decrease infection with SPTBN1 knockdown in the TCN14 microglial cell line, the daughter cell line of the CHME3 cells used in this project.

The second aim of this research is to investigate the role of SPTBN1 on viral fusion. A knockdown of SPTBN1 will be done using the same methods as Aim 1, through siRNA transfection. Synchronized viral fusion will be done by spinoculation of microglial cells with VSV-g HIV-GFP reporter virus. During early time periods after infection, a viral fusion inhibitor will be added to differentiate fused and unfused virus. This addition is done at various times to look at the fusion overtime. The amount of GFP positive infected cells will then be quantified by flow cytometry. It is hypothesized that the knockdown of SPTBN1 will decrease the ability of

VSV-g HIV-GFP to infect microglial cells. The SPTBN1 knockdown has shown varied decreases in infection using different pseudotyped virus within natural host cells and other cell lines. SPTBN1 is an actin organizing protein that was identified in the Brass research as being involved in the HIV infection process when using pseudotyped virus. The study by Gallo contradicted this, showing that the knockdown of SPTBN1 knockdown affected wildtype HIV-1 enveloped virus more severely than VSV-g pseudotyped virus. This will verify if SPTBN1 knockdown decreases infection in VSV-g pseudotyped virus that enters the cell through an endosome rather than at the membrane like wildtype HIV-1.

The third aim of this research is dependent upon the previous aims being complete and time allotted. The third aim is to visualize the disruption, if any, of the actin cytoskeleton and localization of HIV-1 with SPTBN1 knockdown during early replication stages. The siRNA knockdown will used to decrease SPTBN1 expression and cells will be infected with the fluorescently labeled HIV-GFP virus. The cells will be fixed at various times points, stained for the actin cytoskeleton, and visualized by fluorescent microscopy. It is hypothesized that the knockdown of SPTBN1 will disrupt the actin cytoskeleton in a way that changes the localization of HIV-1 within microglial cells. The Dai study used fluorescence microscopy to visualize the disruption of the actin cytoskeleton after SPTBN1 knockdown and determined a decrease in infection. The past work of Marc Havlicek indicated an alteration in uncoating kinetics with knockdown of SPTBN1. Because SPTBN1 is important for organizing the structure of actin, and actin associates with HIV-1 during infection, disruption of actin will likely change the movement of HIV-1 in early replication stages.

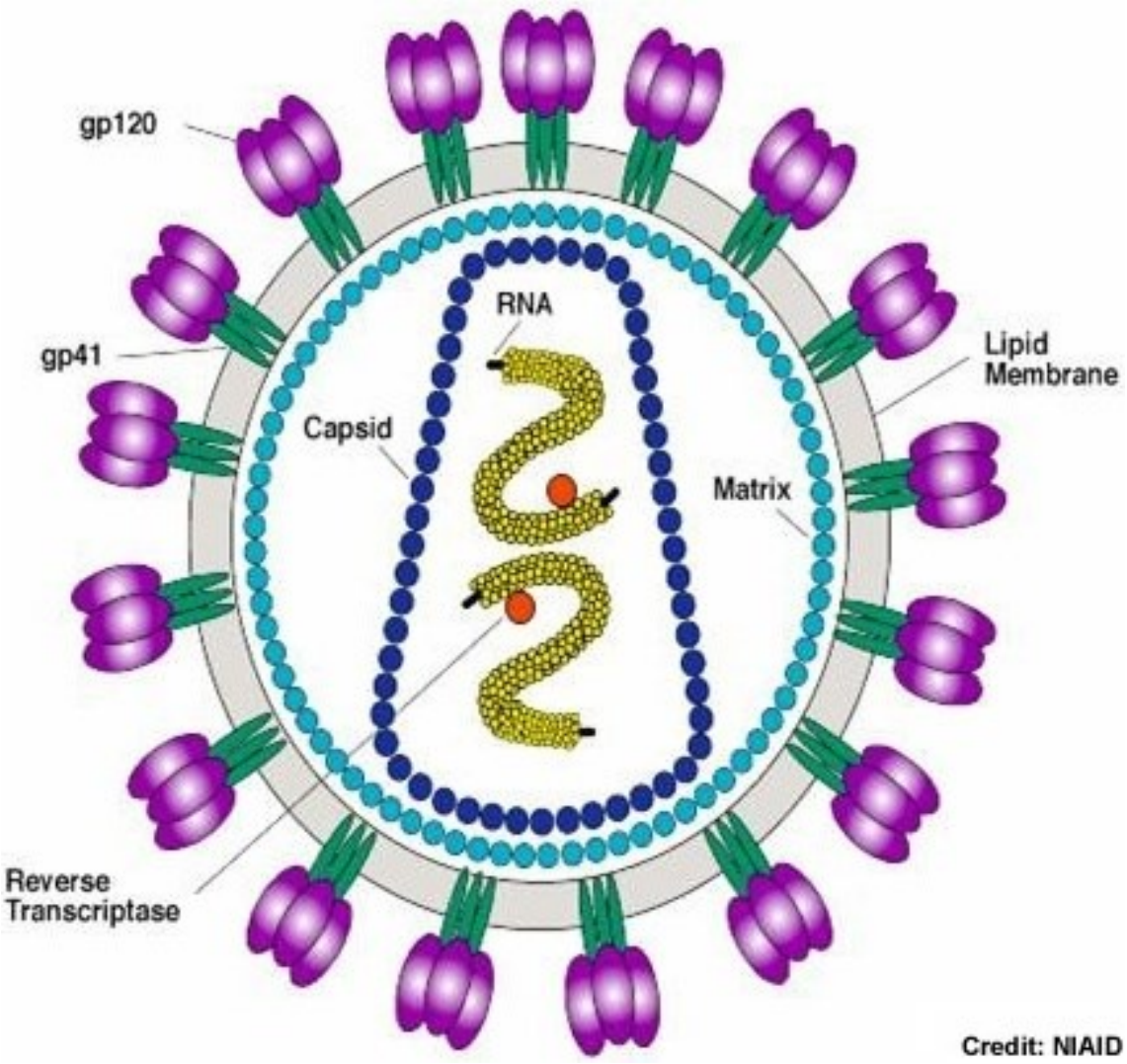

Figure 1. HIV-1 Virion Structure.
The model is a representation of the HIV-1 virion and the placement of the proteins within it. The viral membrane contains the gp120 and gp41 proteins with the matrix protein underneath the membrane. The dark blue circles are the capsid proteins that surround the viral RNA genome in yellow and the reverse transcriptase molecule in red (48).

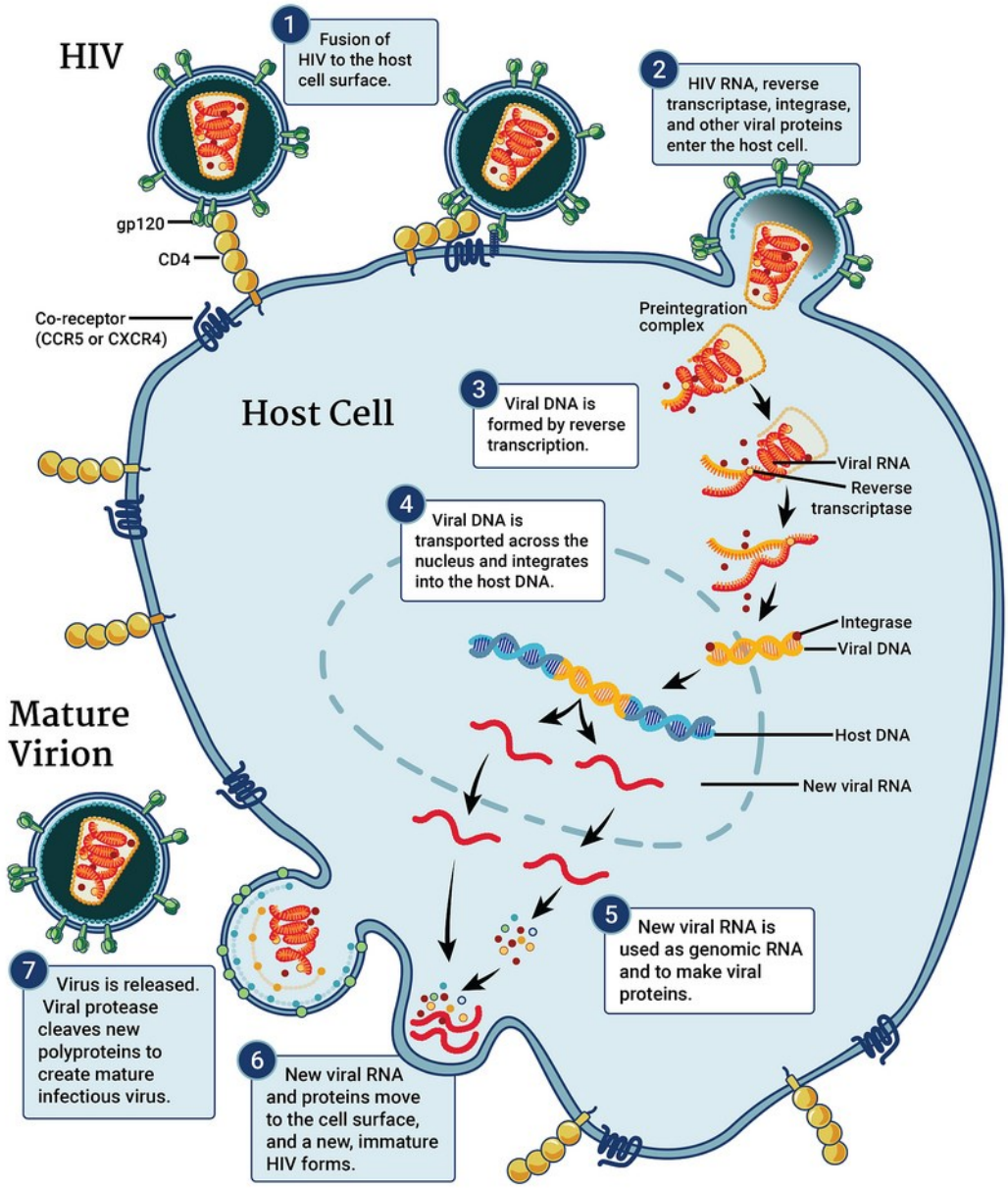

Figure 2. HIV-1 Replication Cycle.
A schematic of the replication cycle of HIV-1 virus. (Step 1) HIV-1 binds to the cost cell via an interaction of the gp120 viral protein and the CD4 host cell receptor. (Step 2) Fusion of the virus and host cell membranes fuse after a conformational change of the receptors. (Step 3) After the capsid is released into the host cell, the capsid undergoes uncoating and reverse transcription of the viral RNA occurs. (Step 4) The viral complex is imported into the nucleus where the viral genome is integrated into the host cell genome. (Step 5) Transcription and translation of the new viral genome occurs. (Step 6) The polyproteins congregate at the host cell membrane bud off. (Step 7) The proteins are cleaved and organized to form the mature virion (48).

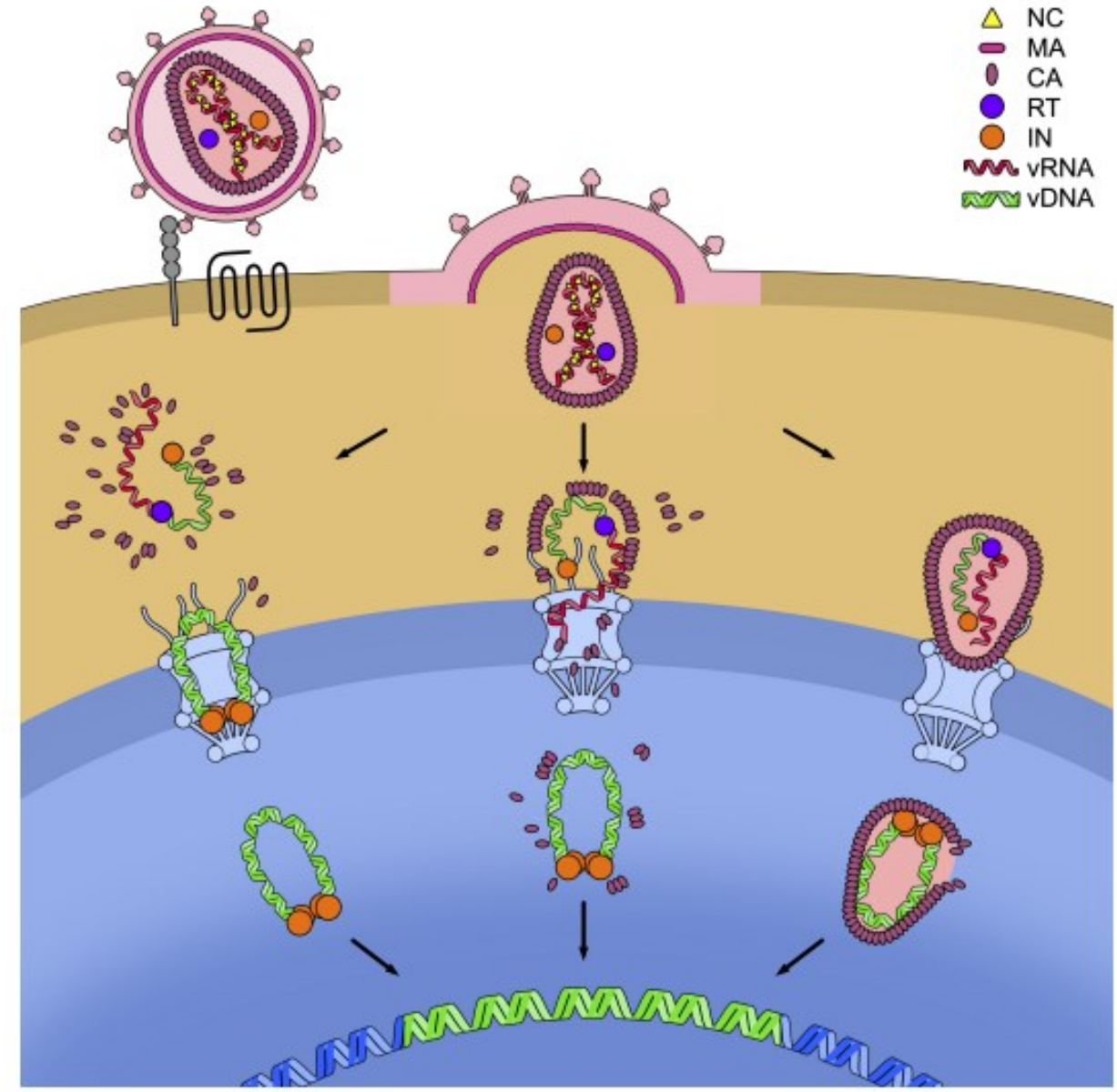

Figure 3. Models of HIV-1 Uncoating.
Three models of HIV-1 capsid uncoating are discussed. The first model is cytoplasmic uncoating where the capsid disassociates slowly as it moves toward the nucleus (left). The second model is the nuclear pore complex (NPC) model where the capsid remains intact until it reaches the nuclear pore (middle). The final model is the nuclear uncoating model where the entire capsid enters the nucleus before uncoating occurs (right; (42)).

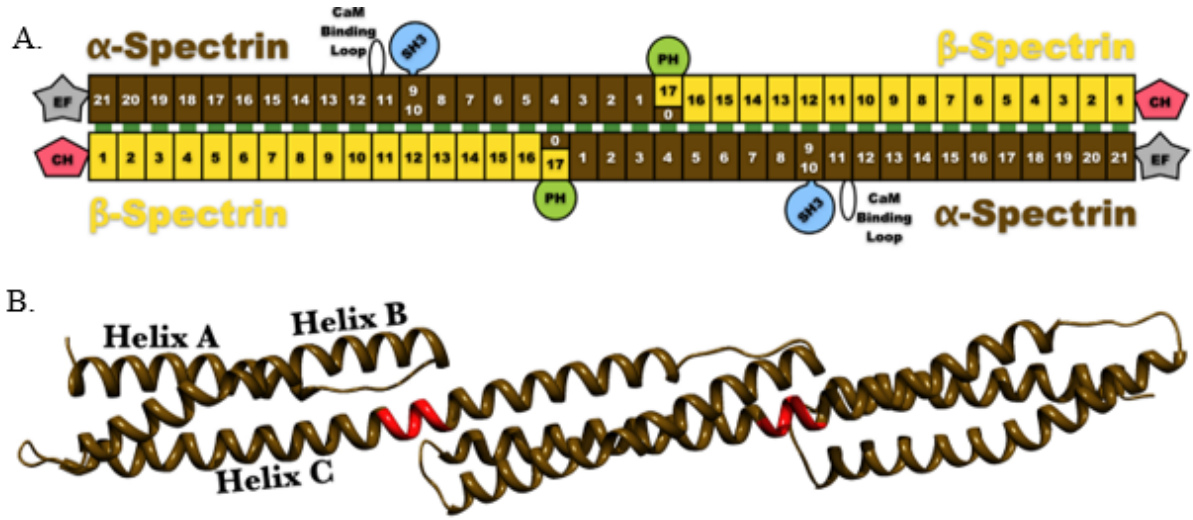

Figure 4. SPTBN1 Structure.
(A) The beta-spectrin molecule is made of four subunits, two alpha (yellow) and two beta (brown) subunits. (B) The tetramer makes helices that interact to create the spectrin network connected by linker sequences (red; (71)).

METHODS

Research Compliance

All research conducted was in accordance with continuing IBC protocols 2022-02.3 and 2022-02.4. The most recent update of these protocols was approved on 02/24/2022 (Appendix A). Institutional Review Board approval was not required for human cell lines used in this research. The 293T HEK cell line, derived from human embryonic kidney cells, was provided by the Hope lab at Northwestern University. The CHME3 cells were a human microglial cell line and provided by the Naghavi lab at Northwestern University (76).

Bioinformatics

Before experimentation could be performed the qPCR primers and siRNA targets were acquired. The primers were ordered from IDT (www.idtdna.com) and tested previously for accuracy of amplification (75). The siRNAs contained a four different sequences in the pools. The siRNAs used were the ON-TARGETplus SPTBN1 pool, GAPDH pool, and non-targeting 4 (NT4) siRNAs were ordered from Dharmacon (Ref# SO-2963171G; horizondiscovery.com; Table 1). Bioinformatics was done to determine the exact location the primers and siRNA target on the specific genes. Using the NCBI database (blast.ncbi.nlm.nih.gov) the GAPDH and SPTBN1 genes were searched and the intron and exon sequence was copied into a word document for highlighting target locations. Each sequence from Table 1 was searched within the document to determine the location the sequences recognized. The forward and reverse primers should be localized to different exons with one intron between them. The primer sequences should be smaller than about 24 nucleotides and have an amplicon size of less than 200 basepairs. The siRNA sequences should be in exons, within different parts across the gene to

ensure an effective knock down. NCBI blast was also done on each sequence to ensure that it was unique to either GAPDH or SPTBN1 genes.

Generating Plasmid DNA to Test Primer Efficiency

The pGEM plasmid has the GAPDH or SPTBN1 sequence inserted. The genes were cloned into the pGEM-T Easy vector (Promega). The plasmids were isolated and used to test the primer efficiency. Each plasmid was transformed into HB101 competent *E. coli* cells (Fig. 5; Promega). The *E. coli* cells were thawed on ice and a 1:100 dilution of the stock plasmid was made. To the thawed cells, 2 µL of the diluted plasmid was added and chilled on ice for 10 minutes. The cells were heat shocked in a hot water bath at 42 °C for 45 seconds before being chilled on ice for 2 minutes. Using sterile technique 900 µL of LB media was added to the cells. The samples were put in the shaking incubator at 220 RPM for 1 hour at 37 °C and LB-Amp plates were prewarmed to 37 °C. After the incubation, 100 µL of the transformed cells were plated on the LB-Amp plates and incubated overnight at 37 °C (77).

Liquid *E. coli* cultures were made from the transformed cultures with 100 mL of LB broth with 100 µg/mL ampicillin concentration (Fig. 5). One colony from the transformation plates was picked up and added to the flask. The cultures were incubated in the ThermoScientific shaking incubator (Model 492) overnight at the same speed and temperature. The plasmid was isolated from the *E. coli* using the Qiagen Plasmid Maxi Kit, according to the Qiagen protocol (Fig. 5; (78)). The centrifugation for 30 minutes was done at 16,000 x g in the ThermoScientific Sorvall RC6+ centrifuge and the sample was filter sterilized using cheese cloth to remove precipitate. The supernatant was put on the equilibrated column and allowed to flow completely through. After the remainder of the protocol was performed, the pelleted DNA was left upside

down on a napkin to remove excess liquid and resuspended in 100 μL elution buffer. The plasmid samples were stored overnight at 4 °C before being moved to -20 °C until used.

The plasmid DNA was verified for the SPTBN1 and GAPDH genes by PCR and restriction digest procedures (Fig. 5). PCR was done with the Maxiprep plasmid DNA, and the appropriate primer set (refer to qPCR methods). The samples were then electrophoresed on a 1% agarose gel with a 100 bp ladder as reference. As PCR controls, the previously used plasmid DNA that was isolated via miniprep was electrophoresed as a positive control along with a water sample with no DNA added as the negative control. Restriction digest was done using *EcoRI* (New England Biolabs) and the samples were run on a 1% agarose gel with a 100 bp ladder. Once verified the plasmid DNA was stored at 4 °C for future use.

Maintaining 293T HEK Cells

The 293T HEK cell cultures were maintained on 10 cm tissue culture plates (Corning) with enriched Dulbecco's Modified Eagle Medium (DMEM; Ref# 10-017-CV), stored at 37 °C and 5% CO_2. DMEM++ media was made with 500 mL of DMEM (Corning) warmed in the 37 °C water bath. Added to this was room temperature, 5 mL of 100X penicillin-streptomycin-glutamine (PSG; Corning; Ref# 30-009-Cl) and 50 mL of fetal bovine serum to make 10% (FBS; R&D Systems). The media was kept sterile by doing the procedure in the tissue culture hood and stored at 4 °C.

To split cells, the media was warmed to 37 °C in a hot water bath and the trypsin (0.05% trypsin, 0.53 mM EDTA, 1X sodium bicarbonate; Corning Ref# 25-052-Cl) was set out at room temperature. In the tissue culture hood, all materials were wiped down with 70% ethanol. An existing 293T cell culture plate was used to make a new culture of cells. The old media was

aspirated off the cells and 1 mL of trypsin was added slowly to the side of the tissue culture plate. The plate was gently tipped to ensure the trypsin covered the entire surface. The trypsin was aspirated off the cells and one more milliliter of trypsin was added to the side of the plate. The trypsin was aspirated off the cells and the plate of cells was placed in the 37 °C incubator for 2 minutes. While incubating, a new 10 cm plate was labeled. The trypsinized plate was removed from the incubator and 10 mL of DMEM++ media was washed over the plate and pipetted up and down gently to dislodge and break up clumps of cells. From the old plate, 1 mL of the cells was added dropwise to the new plate with 10 mL of media. The new plate was gently rocked to disperse the cells and placed back in the incubator. The remaining cells in media on the old plate were aspirated off and the plate was placed in the tissue culture waste. The cells were maintained at 60% to 80% confluence, with a new plate of cells being made if the cells were between that range to keep a proper growth environment.

Making HIV-VSVG-GFP Virus

Virus was made in 293T cells using HIV-GFP and VSV-g plasmids, provided by the Hope lab at Northwestern University. In 1 mL of DMEM media, 6 μg of the HIV-GFP plasmid and 4 μg of the VSV-g plasmid was added along with 40 μL of the transfection reagent polyethylenimine (PEI; Polysciences) and mixed. The mixture was incubated at room temperature for 15 minutes before being added dropwise to an 80% confluent plate of 293T cells. The cells were put in the incubator and the next day, the media was changed to 10 mL of fresh DMEM++ media.

The virus produced from the cells was harvested two days after transfection in the culture hood. A 45 μm filter (Millapore Sigma) was attached to a 20 mL syringe with the plunger

removed. The filter was placed over a 50 mL conical tube and the media from the cells was poured into the syringe with the filter attached. The plunger was replaced, slowly depressed to filter all the media. The media from the 50 mL conical tube was stored in cryovials in 1 mL aliquots at -80 °C.

Maintaining CHME3 Cells

CHME3 cells were maintained on a 10 cm tissue culture petri dish with CHME3 media kept at 37 °C and 5% CO_2. CHME3 media used 500 mL of DMEM warmed to 37 °C, 25 mL of FBS to make 5%, 1X PSG, and 5 mL 100 mM sodium pyruvate at room temperature (Corning).

To split cells, the CHME3 media was warmed in a 37 °C water bath and the trypsin was set out at room temperature. The tissue culture hood and all materials were wiped down with 70% ethanol prior to the procedure. A plate of CHME3 cells was retrieved from the incubator to make a new plate of cells. The cells were put into a new culture when at 60% to 80% confluence. The old media was aspirated off the cells and 5 mL of 1X PBS was added to the side of the plate. The PBS was aspirated off the cells and 3 mL of trypsin was added to side of the plate. The plate was placed back in the incubator for 2-3 minutes. A new plate was labeled and 10 mL of CHME3 media was added. The plate was retrieved from the incubator and gently tapped on the sides to remove the cells from the bottom. In the tissue culture hood, 7 mL of CHME3 media was added to the plate of cells and trypsin. The media was washed over the plate and pipetted up and down to remove clumps of cells. From the old plate, 1.5 mL of cells in media was added dropwise to the new plate with the media on it. The plate was gently rocked to disperse the cells and placed back in the 37 °C incubator. The remaining cells in media from the old plate was either used for plating cells for an experiment or aspirated off and the plate was discarded in the tissue culture waste.

Procedure for Plating Cells for siRNA Transfection

The CHME3 cells were maintained as explained previously and the extra cells were used to plate in a 6-well plate. A hemocytometer was wiped off with ethanol and allowed to dry. The cells remaining from an old plate were put in a conical tube. The tube was inverted three times and 15 μL of the cells were removed and placed on the hemocytometer. The Olympus CKX41 microscope was used to count all four quadrants that were averaged together and multiplied by the dilution factor of 10,000 (79). The desired number of cells in each well for transfection was 1.7×10^5 cells in each well for a 6-well plate which was multiplied by the number of wells needed. The total number of cells needed was divided by the number of cells in the remainder from the plate of cells. The calculated value was the volume of the cultured cells needed in a total volume equal to the number of wells plated times two. CHME3 media was added to the cultured cells to volume. The tube of cells in media was inverted and 2 mL of the solution was added to each well of a 6-well plate. The plate was gently rocked back and forth and placed in the incubator.

siRNA Transfection Protocol

A day after the cells were plated in a 6-well plate, an siRNA transfection was done. The cells were checked to be 60-80% confluent before transfection. The tissue culture hood was wiped down with RNAaseZap (Invitrogen) as well as the p20, p200, p1000, rack for tubes, and marker. The pipettes with tips and microcentrifuge tubes were placed in the tissue culture hood and the hood was exposed to UV for 15 minutes. The GAPDH, SPTBN1, and NT (non-targeting 4) RNA duplexes (Dharmacon) were thawed on ice and the OPTIMEM (Corning) and Lipofectamine RNAiMAX (Invitrogen) reagents removed from 4 °C to be warmed to room

temperature. The siRNA transfection was performed in the hood, starting with two Eppendorf tubes for each sample. The transfection reagent and siRNAs were diluted with media with the following amounts, tube 1 had 50 μL of OPTIMEM with 4 μL of lipofectamine RNAiMAX added. In tube 2, 100 μL of OPTIMEM was combined with 3 μL of either GAPDH, SPTBN1, NT, or no siRNA for a 100 pmol concentration, and the tubes were gently tapped to mix. These volumes were used for one reaction in one well. Both tubes were incubated at room temperature for 5 minutes. The tube 1 content was added to the tube 2, mixed by pipetting, and incubated at room temperature for 20 minutes.

The media on the cells was aspirated off and 1 mL of OPTIMEM was added to the side of each well. The siRNA mixture was added to the appropriately labeled well dropwise. The plate was gently rocked back and forth and placed in the incubator. Four hours after the transfection the media on the cells was aspirated off and 1 mL of DMEM without PS, warmed in the 37°C water bath, was added to the side of the well. The next day the media was aspirated off and 2 mL of warmed CHME3 media was added to the side of each well for later RNA isolation or replated into a 96-well plate for infection.

New Lipofectamine RNAiMAX Transfection Protocol

The day before transfection, the cells were plated to have 60-80% confluency at transfection. The tissue culture hood, p10, p20, p200, p1000, rack for tubes, and marker were wiped down with RNAaseZAP and placed in the hood. The microcentrifuge tubes and pipette tips were placed in the hood before exposing it to UV for 15 minutes. The RNA duplexes, SPTBN1, GAPDH, and NT were thawed on ice. The OPTIMEM and lipofectamine were removed from the fridge. CHME3 media was warmed to 37 °C. The transfection procedure was

done according to the standard Lipofectamine RNAiMAX transfection protocol from Invitrogen for 2.5 x 10^5 cells per well. The stock of the RNA duplexes was 20 μM with 1.5 μL used to make the 30 pmol concentration (80). The cells were replated the following day into a 96-well plate for infectivity and one 6-well plate was used for RNA harvesting two days after transfection to determine SPTBN1 expression.

RNeasy RNA Purification

Total RNA was isolated and purified from the transfected CHME3 cells using the Qiagen RNeasy Plus Mini kit and protocol (78). The media was removed from the transfected cells and 1 mL of 1X PBS was added to the side of the well. The PBS was aspirated off and an in-well lysis was performed using a mixture of 10 μL β-mercaptoethanol for each 1 mL of RLT buffer. For the 6-well plate, each well received 350 μL of the buffer RLT-β-mercaptoethanol solution. The solution was left to sit briefly before the tip of a pipette was used to dislodge the cells from the surface of the wells. The cell solutions were added to a microcentrifuge tube and homeogenized by vortexing breifly. The lysates were pipetted onto a QIAshredder spin column to homogenize the sample. The run through was transferred to a gDNA Eliminator column to remove gDNA. Into the collection tube with the run through, 350 μL of 70% ethanol was added, and the procedure continued. After the wash procedures, the run through was discarded in the waste container and a new collection tube was placed on the column to remove any extra wash buffer. The RNA was eluted off the column with the addition of 50 μL of nuclease-free water. The columns were discarded, and the samples were placed in the -20°C freezer until PCR was performed.

SsoFast qPCR

The Bio-Rad SsoFast EvaGreen qPCR Supermix procedure was compared to the iTaq One Step Kit for earlier detection and accuracy (81, 82). The SsoFast reactions were 20 μL each including 0.5 μM each of the forward and reverse primers and 1 μL of the DNA sample (Table 1). The thermocycler used was a Bio-Rad CFX model with the parameters set in the protocol (81). The initial holding stage was 95 °C for 30 seconds before the cycling began. The cycle stage of qPCR contains two steps, one at 95 °C for 5 seconds and one at 60 °C for 5 seconds. The plate was read after each cycle to determine at what cycle PCR product was amplified. The cycle number that product was amplified was the C_T value. The cycling stage was repeated 45 times (Fig. 6). After all the cycles are complete there was a melt curve as the final step that determines at what temperature the product strands melt from each other. The desired products should have the same melting temperature and was used to verify no contamination (Fig. 6).

iTaq One Step qPCR

Quantitative PCR (qPCR) or quantitative reverse transcription PCR (qRT-PCR) was performed using the Bio-Rad iTaq Universal SYBR Green One Step Kit protocol (82). The reaction totals were 20 μL each including 1 μL sample DNA or RNA and 0.3 μM each of the forward and reverse primers, either GAPDH or SPTBN1, as well as the supermix (Table 1). The thermocycler used was a Bio-Rad CFX model with the parameters set in the protocol. The reverse transcriptase step was at the beginning of the qPCR procedure being 50 °C for 10 minutes to make the RNA sample into cDNA. The holding stage was 95 °C for one minute. The cycling stage included two steps, one at 95 °C for 10 seconds and one at 60 °C for 30 seconds. The cycle was done 45 times and a melt curve was added at the end the same as the SsoFast

protocol (Fig. 7). This procedure was done for determining the knockdown amount and the primer efficiency.

Pfaffl Method to Analyze qRT-PCR

Primer efficiency was performed by doing qPCR with seven dilutions of genomic DNA to make a standard curve. The Pfaffl efficiency and quantification of knockdown was done as described in the Essential Laboratory Techniques (Unit 10.3.33, Current Protocols; (83)). The Pfaffl efficiency was determined using the slope of the standard curve plus one (Fig. 8). The Pfaffl method uses the change in C_T value determined by subtracting the experimental C_T value from the non-targeting control C_T value. The Pfaffl efficiency was taken to the power of the change in C_T value of the gene to determine the fold change between samples. The fold change between the target samples (SPTBN1) were divided by the fold change of the housekeeping gene (GAPDH) samples. This determined the normalized fold change of the knockdown (Fig. 18).

Infecting with Virus

The day after the CHME3 cells were transfected with siRNAs, the cells were replated in a 96-well plate. The procedure on the 6-well plate was the same as maintaining the CHME3 cells with washes of 1X PBS before the cells were trypsinized. Once the cells were removed from the bottom of the plate, each separate transfection reaction was put into a conical tube. Using a hemocytometer, the cells were counted, and the calculation was done to determine the volumes of cells and media needed to plate 6,000 cells in each well of a 96-well plate. The cells were plated for the number of reactions to be performed and the plate was put back in the incubator.

The following day, the cells were infected with virus. A dilution series of virus was done initially to determine the proper virus concentration to use. Before the virus was added, the

media on the cells was changed to CHME3 media soon after removed from 4 °C fridge, with 1 µL polybrene for every 2 mL media (1X). The first reaction wells were changed to CHME3 media with 1 µL polybrene for every mL media (2X). From the thawed virus vial, 100 µL was added to the first row that had the 2X polybrene media. A serial dilution was made by adding 100 µL from the first well to the next well and so on, leaving the last two wells without virus as negative infection controls. The plate was then spinoculated in the ThermoScientific centrifuge (Ref: 75004261) at 1,200 x g at 16 °C for one hour to synchronize infection. Immediately after the centrifugation was completely, the media was replaced on all the wells to 200 µL CHME3 media and the plate was placed back in the incubator. The next day the media was replaced again with CHME3 media at 37 °C.

The final day was fixing the cells before flow cytometry could be done. The media on the 96-well plate was removed and cells were washed with 1X PBS. The cells were trypsinized with 100 µL and put in the incubator for 5 minutes, until the cells came off the bottom of the well. The cells were resuspended in the trypsin. The cells were fixed using 100 µL of a 1:1 paraformaldehyde and 1X PBS solution. The plate was parafilmed, covered in aluminum foil, and put at 4 °C until flow cytometry.

Flow Cytometry to Deterime Viral Infectivity

Infectivity was assessed by flow cytometry to find the percent GFP positive cells that indicated HIV-GFP infection. Each well was resuspended before flow cytometry was performed. The software was turned on and instructions followed on the Accuri C6 flow cytometer (BD Biosciences). The template was selected with the parameters set to 10,000 events or 80 µL limit, and fast run speed. As each sample was tested, they were named based on the virus dilution and siRNA transfection reaction. Plot 1 of the template displayed the live cell count and the

percentage of particles that were live cells as opposed to cell debris. Plot 2 of the template displayed the percent of the cells that expressed GFP. After all samples were run, the uninfected or no virus samples for each siRNA transfection condition were used to set the GFP fluorescence threshold to between 0.01-0.0%. In an excel file the data was collected to have plot 1 as percent and count of live cells and plot 2 had percent of infected cells. After all samples, the flow cytometer was shut down based on the instructions.

Viral Fusion Assay

A viral fusion, ammonium chloride add-in assay was done to determine the amount of fusion overtime. An initial fusion assay was done with various concentrations of ammonium chloride, 10 mM, 25 mM, 50 mM, and 100 mM. CHME3 cells were plated at 6,000 cells per well on a 96-well plate. The following day, the cells were infected in the presence of ammonium chloride. A $1/100^{th}$ dilution of virus was used with the ammonium chloride concentrations in CHME3 media also containing 1X polybrene. The media and virus media were placed on the cells and spinoculation was performed to synchronize fusion at 16 °C 1200 x g for 1 hour. After the spin, the media on the cells was changed to CHME3 media with the corresponding ammonium chloride concentration. The next day the media was changed to CHME3 media without ammonium chloride. The cells were harvested as previously described in the infecting with virus section. Flow cytometry was performed as described in the testing infectivity section of the methods to determine the number of cells infected with the various concentrations of ammonium chloride.

The following fusion assays used the 10 mM ammonium chloride (NH_4Cl) concentration. Master mixes were made for the constant NH_4Cl samples and no virus controls. The corresponding media mix was added to the samples, all other wells had CHME3 media with

virus and polybrene as previously stated. The plates were spinoculated and immediately after removing from the centrifuge the media on the wells was changed to 200 μL CHME3 media or 10 mM NH_4Cl CHME3 media for the NH_4Cl constant reaction and 0 hour time point. At 15, 30, 45 minutes, 1, 2, 3, and 4 hours following infection, the media on the corresponding wells was changed to NH_4Cl media. In between time points the plates were kept in the 37 °C incubator and the NH_4Cl media was warm in the 37 °C bead bath. The following day all of the media on the samples was removed and replaced with 100 μL CHME3 media. The cells were harvested as previously described two days following infection and stored at 4 °C until flow cytometry was performed.

Half-life Calulations

Fusion assay results were normalized to the maximum infection of that siRNA transfection reaction and was used to determine the half-life of fusion. To find the half-life time, the two time points on either side of 50% were graphed separately. An equation of the line made by those points was found and 50 was plugged in for y. The value of x was solved for and indicates the time in hours it took for half of the HIV virus to fuse with the cells in that sample. This hour time was converted to minutes and seconds. An average time from three independent experiments was found and a two tail independent t-test was done to determine if there was a statistical significance between the half-life of HIV fusion in SPTBN1 and NT siRNA transfected cells. The analysis was done through SPSS comparing the fusion half-life times for the SPTBN1 and NT knockdown samples.

Table 1. Primer and siRNA Sequences

Sequence	SPTBN1	GAPDH	Non-targeting
Forward Primer	GCACACTACATTTGAGCATGAC	GCACCGTCAAGGCTGAGAAC	N/A
Reverse Primer	GTTCTCGCGCTTCTGGATA	GCCTTCTCCATGGTGGTGAA	N/A
siRNA Target 1	CGGAAGAGAUCGCCAAUUA	GUCAACGGAUUUGGUCGUA	N/A
siRNA Target 2	GACGAGAUCUUGUGGGUUG	CAACGGAUUUGGUCGUAUU	N/A
siRNA Target 3	CUUAUGUGGUGACUUAUUA	GACCUCAACUACAUGGUUU	N/A
siRNA Target 4	CGAGUGCAAUGAAACCAAA	UGGUUUACAUGUUCCAAUA	AUGAACGUGAAUUGCUCAA

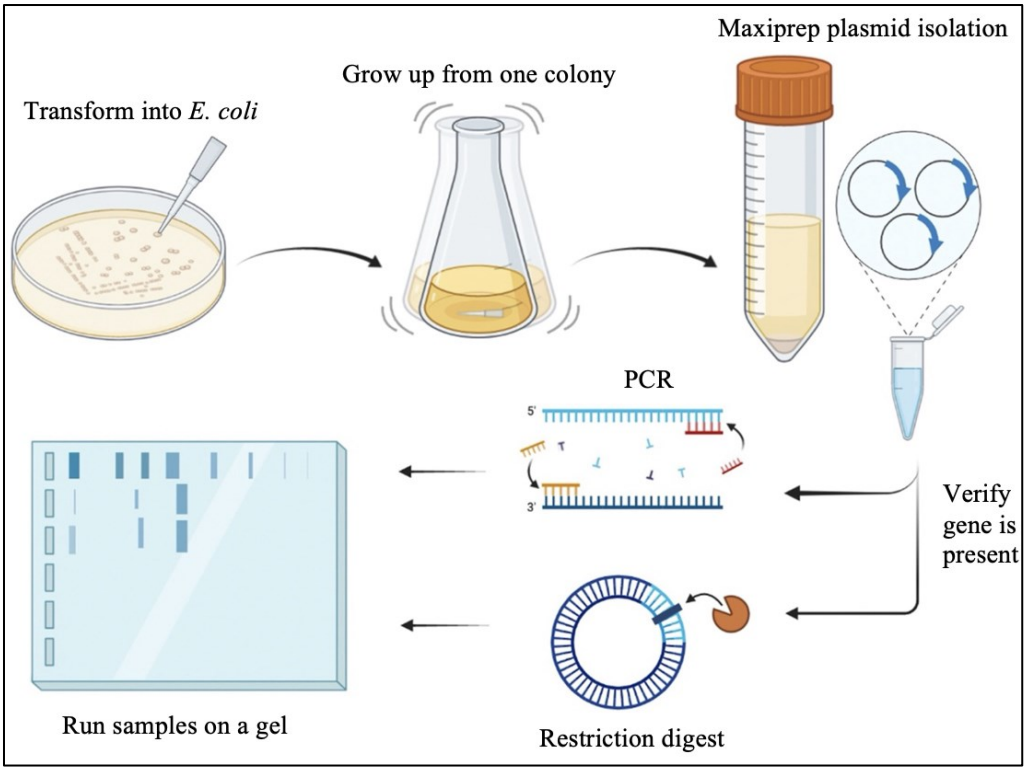

Figure 5. Growing up new plasmid DNA.
Plasmid DNA with either GAPDH or SPTBN1 gene present was transformed into competent *E. coli,* grown in liquid media in the presence of an antibiotic, and from that culture the plasmid DNA was isolated via Maxiprep. The plasmid DNA was confirmed for the genes by restriction digest and PCR that was run on a gel.

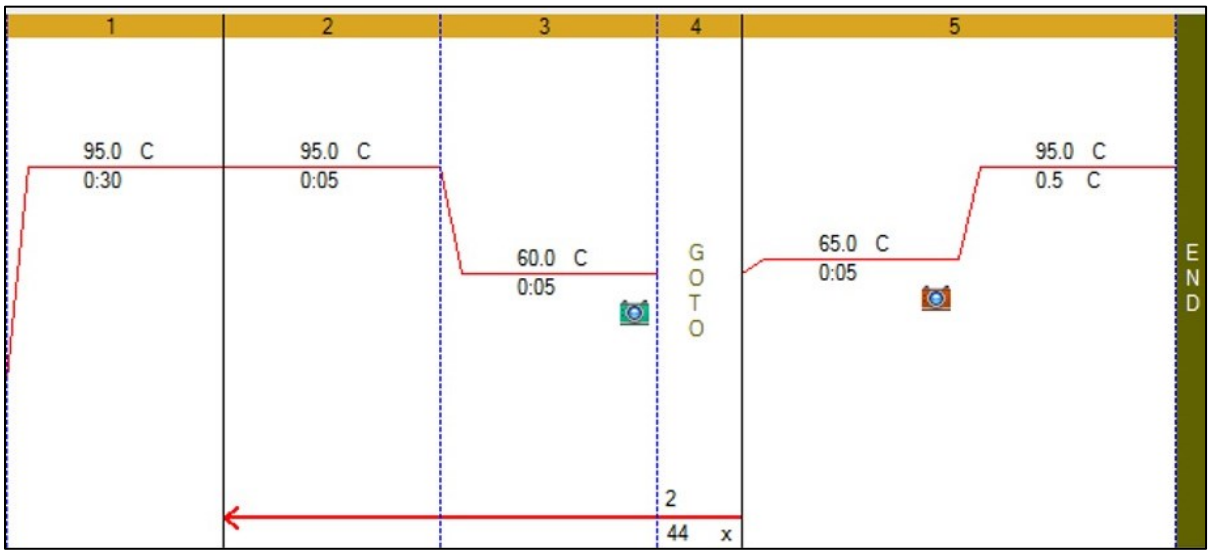

Figure 6. SsoFast EvaGreen Protocol.
The qPCR protocol was set up and ran on a Bio-Rad CFX thermocycler included a holding stage and cycle stage to amplify the desired product. Screen grab from Bio-Rad COX manager software.

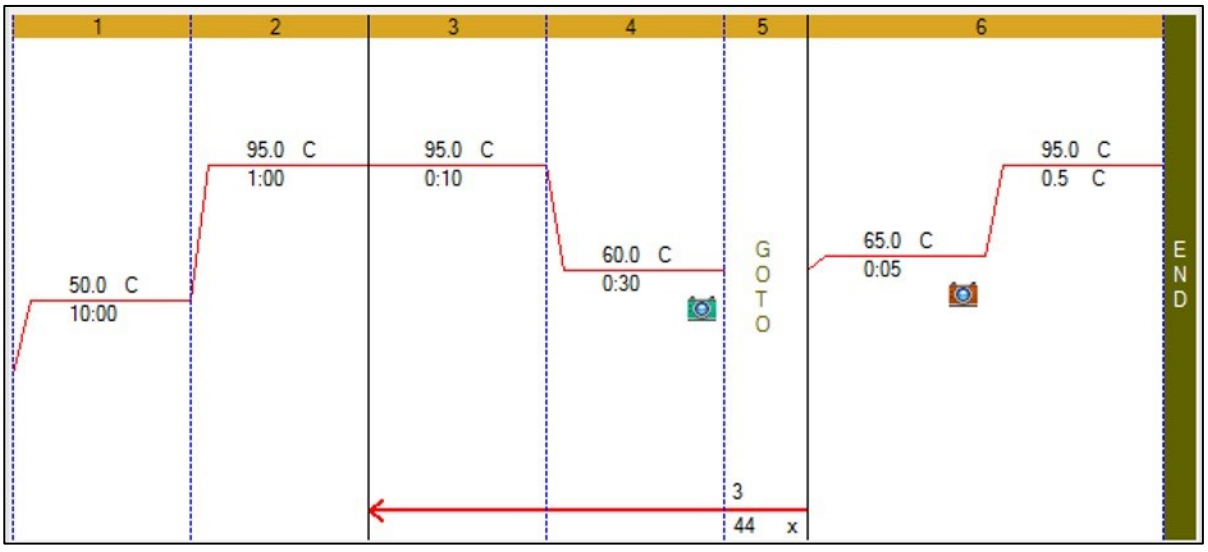

Figure 7. iTaq SYBR Green Protocol.
The qPCR was performed on a Bio-Rad CFX thermocycler. This protocol included a reverse transcription step, holding stage, cycling stage, and a melt curve procedure. Screen grab from Bio-Rad COX manager software.

$$\text{Normalized Fold Change} = (E_{p\text{-target}})^{\Delta CT\text{-target}} / (E_{p\text{-housekeeping}})^{\Delta CT\text{-housekeeping}}$$

$$\text{Pfaffl Efficiency } (E_p) = \text{Primer efficiency} + 1$$

$$\text{GAPDH primer efficiency} = 0.62$$

$$\text{SPTBN1 primer efficiency} = 0.79$$

$$C_{T\ control} - C_{T\ experimental} = \Delta C_T$$

$$\text{Fold change between samples} = (E_p)^{\Delta CT}$$

Figure 8. Pfaffl Knockdown Calculation.
The equation to determine the normalized fold change of gene expression is stated. The primer efficiency based on the iTaq Universal SYBR Green One-Step Kit for GAPDH and SPTBN1 primers is 0.62 and 0.79 respectively (see primer efficiency results).

RESULTS

Bioinformatics

Bioinformatics using NCBI was done to determine where the primers and siRNAs targeted within the SPTBN1 and GAPDH genes. SPTBN1 has 36 exons (Fig. 9A) with the siRNAs targeting exon 8 (blue), exon 14 (orange), exon 16 (green), and spanning exon 21 and 22 (purple; Fig. 9B). The forward primer for SPTBN1 binds at the end of exon 26 and the reverse primer binds within exon 27 (Fig. 9C). The qPCR primers amplify a sequence of 127 basepairs. NCBI Blast of siRNA and primer sequences indicate uniqueness to SPTBN1 mRNA transcript 1.

Bioinformatics was done on the GAPDH gene in the same manner as SPTBN1. GAPDH has 9 exons with siRNAs targeting four locations (Fig. 10A and B). Two siRNAs spanned two exons, exon 2 and exon 3 (blue and purple). Another siRNA targeted an area in exon 3 (green) and one in exon 4 (orange; Fig. 10B). The forward GAPDH primer recognizes a sequence in exon 4 and the reverse primer recognizes exon 5 (Fig. 10C). The qPCR primers amplify a sequence of 151 basepairs. NCBI Blast of the GAPDH primer and siRNA sequences showed they were unique for GAPDH mRNA transcript 1.

qRT-PCR Protocol

Two qRT-PCR protocols were compared, SsoFast EvaGreen Supermix that was used previously and iTaq Universal SYBR Green One-Step Kit, a new kit. To quantify RNA samples, qRT-PCR was preformed to get a quantitative cycle number (C_q) that represents at what cycle the sample was amplified. The qRT-PCR protocol was optimized because it was done in all future experiments. A serial dilution of plasmid DNA and no DNA control was used with both qPCR kits to determine which protocol to use. The qPCR was done with the SPTBN1 and

GAPDH primer sets. A smaller C_q value indicates the sample was amplified at a lower cycle number. The iTaq One-Step Kit amplified the plasmid DNA three cycles sooner for both primer sets (Table 2). The iTaq One-Step Kit had greater C_q values in the no DNA sample which was the background level of amplification. Because the earlier amplification of the sample and less background with the iTaq One-Step Kit, it was used for the remainder of qRT-PCR procedures. With the protocol determined, the primer efficiency with the kit had to be determined.

Primer Efficiency

The primer efficiency of SPTBN1 and GAPDH primer sets was determined using plasmid DNA dilutions and qPCR. A serial dilution of the plasmid DNA with SPTBN1 sequence was made with seven dilutions. The DNA dilutions were quantified by qPCR in triplicate. The initial dilutions made were 5 μL of plasmid DNA in 45 μL water. The results were not evenly spread which is desired of a serial dilution (results not shown). Because the results were not what is expected from a serial dilution. A larger dilution volume was used.

The second dilution of plasmid DNA made used 20 μL sample in 180 μL water with the qPCR results shown in the amplification curves (Fig. 11). The C_q values of five dilutions was used to make the standard curves (Table 3 and Fig. 12). The standard curve shows the equation of the line and the R^2 value that indicates how well the equation represents the data. An R-squared value above 0.99 was desired to show the equation was accurate. The equation [10^(-1/slope) -1] was used to determine the primer efficiency. The same procedure was done in duplicate to verify the results. The first run had a primer efficiency of 0.55 and the second run had a primer efficiency of 0.53.

The calculated primer efficiencies for SPTBN1 with the iTaq One-Step Kit (0.53 and 0.55) were much lower than the primer efficiency with the SsoFast EvaGreen supermix kit used previously in the lab, obtained by Marc Havlicek (1.05). Due to the lower efficiency, optimization was done to increase the primer efficiency. The SPTBN1 primer sets were rediluted from the stock primers and used at a higher concentration to ensure the primer amount was not limiting the sample amplification. The primers were being used at 0.3 μM concentration and this was increased to 0.5 μM concentration. The standard curve from this data was not the desired result (Fig. 13). The R^2 value was low at 0.8178 meaning that the equation for the line could not be trusted.

Next, the plasmid DNA was regrown and isolated for the serial dilution. The plasmid DNA was transformed into *E. coli,* grown up in liquid culture, isolated using a Maxiprep, and verified by PCR and restriction digest. The PCR was performed with the SPTBN1 and GAPDH primers on the previous plasmid DNA (mini), the newly isolated plasmid DNA (maxi), and a water sample as a negative control (Fig. 14). The SPTBN1 primers should amplify a product of 127 basepairs and the GAPDH primers should amplify a product of 151 basepairs. The SPTBN1 mini and maxi samples had product amplified between 100 and 200 basepairs as compared to the known ladder. The GAPDH mini and maxi samples had product between 100 and 200 basepairs and was slightly higher on the gel than the SPTBN1 products (Fig. 14). Based on the PCR results, the SPTBN1 and GAPDH sequences were within the plasmid DNA.

A restriction digest was also done to further confirm the genes in question were present. There were cut sites for the EcoR1 restriction enzyme on either side of the inserted genes, SPTBN1 and GAPDH. The product sizes were expected to be the same as the PCR products. The SPTBN1 sample had product between 100 and 200 basepairs. The GAPDH sample had product

slightly higher than the SPTBN1 on the gel meaning the GAPDH product was slightly larger than SPTBN1 (Fig. 15). This was a second verification that the SPTBN1 and GAPDH genes were within the newly isolated plasmid DNA. This plasmid DNA was used for the remainder of the primer efficiency experiments.

With the new plasmid DNA verified for the SPTBN1 and GAPDH genes, the primer efficiency procedures were continued. A new 1:10 dilution series of the SPTBN1 plasmid DNA was done as previously. The qPCR results of two runs of the new plasmid DNA dilution had a calculated primer efficiency of 0.84 and 0.74 (Table 4). These runs had efficiencies closer to the previously calculated SsoFast primer efficiency. An average of the two runs was 0.79 and used as the SPTBN1 primer efficiency for determining knockdown of the gene.

The GAPDH primer efficiency was determined with the same procedure as the SPTBN1 primer efficiency using the GAPDH primer set with the plasmid DNA from the Maxiprep (Fig. 14 and 15). The Cq values for the five dilutions were used to make a standard curve (Table 5 and Fig. 16). The qPCR of the serial dilution was done twice to verify the results. Each time the standard curves had R-squared values greater than 0.99 (Fig. 16). The primer efficiency for both runs was 0.62 (Table 5 and Fig. 16). Because both runs had the same calculated efficiency, the GAPDH primer efficiency of 0.62 was used for the knockdown calculations.

Comparison of Two siRNA Knockdown Protocols

After the primer efficiencies were calculated, siRNA knockdowns of SPTBN1 were performed. Knockdown of SPTBN1 was performed by siRNA transfection to decrease the expression of the protein. Knockdown was also done on GAPDH initially to verify the procedure worked to decrease protein levels. Following siRNA knockdown, the RNA was isolated from the cells and quantified by qRT-PCR using SPTBN1 and GAPDH primers. The qRT-PCR curves

indicate at what cycle the RNA product was amplified and represents the amount of RNA product present in each sample (Fig. 17). Based on what cycle the samples were amplified, the change in expression of SPTBN1 can be determined using the Pfaffl calculation method with primer efficiencies previously determined.

The Pfaffl method compares the change in RNA levels of a gene in question to a housekeeping gene (like GAPDH) where the levels should not change. Two siRNA knockdown protocols were compared to determine the most efficient procedure, with the greatest decrease of SPTBN1 RNA. The change in SPTBN1 RNA level was determined by subtracting the cycle number (C_T) that SPTBN1 primers amplified product in the SPTBN1 knockdown experiment from the non-targeting siRNA experiment (Fig. 18). The Pfaffl efficiency was used as the base to the power of the change in C_T value. This calculation was done with both SPTBN1 and GAPDH primer sets. The normalized RNA fold change was calculated by dividing the end value for the SPTBN1 primers by the GAPDH end value. This represents the percent expression as a decimal of SPTBN1 (Fig. 18).

The expression level of SPTBN1 was determined using the method described above for two siRNA knockdown protocols. A protocol used by previously in Dr. Hulme's lab was designated the old knockdown protocol and the RNAiMAX protocol was designated the new knockdown protocol. The old knockdown protocol resulted in 83.5% expression of SPTBN1, and the new protocol resulted in 11.5% expression of SPTBN1 (Fig. 18 and 19). This can also be stated as the old protocol caused a 16.5% decrease of SPTBN1 expression while the new protocol caused an 88.5% decrease of SPTBN1 expression. The new siRNA knockdown protocol was more efficient at knocking down SPTBN1 compared to the old knockdown protocol. A greater decrease of SPTBN1 expression was desired to see the effect of the absence of SPTBN1.

Therefore, the new protocol was used when determining the change in infectivity after siRNA knockdown.

Effect of SPTBN1 Knockdown on HIV Infectivity

The new siRNA knockdown protocol was performed on CHME3 cells to decrease SPTBN1 expression, after which the cells were infected with HIV. Previous publications show that SPTBN1 knockdown decreases HIV infection with varying significance depending on the cell types and virus used (56, 68, 74). The new knockdown protocol was performed twice with infection afterwards. The expression of SPTBN1 in the first infectivity assay was 29% or a 71% decrease of expression (Fig. 20). The cells were infected with eight dilutions of HIV-GFP virus and infectivity was determined by flow cytometry (1/2, 1/4, 1/8, 1/16, 1/32, 1/64, 1/128, and 1/256). The infectivity results were normalized to the non-targeting siRNA knockdown control at 100%.

The first knockdown (10/13/21) and infectivity experiment resulted in infection after SPTBN1 knockdown remaining relatively the same as the non-targeting knockdown. The $1/8^{th}$ and $1/16^{th}$ dilutions had slight decreases in infection. The $1/64^{th}$, $1/128^{th}$, and $1/256^{th}$ dilutions had slight increases in infection after SPTBN1 knockdown and the remaining dilutions had the same amount of infection (Fig. 21). The same procedure was repeated to verify the results.

The second siRNA knockdown with the new protocol (10/26/21) had 7% expression of SPTBN1 or 93% decrease expression (Fig. 20). This was the greatest decrease in SPTBN1 expression that the new knockdown procedure achieved. The infectivity results showed that at every dilution of virus, infectivity increased with the SPTBN1 knockdown compared to the non-targeting knockdown (Fig. 22). This was the opposite of previous published results and what the

previous graduate student achieved with the old siRNA knockdown protocol. Because of this, the old knockdown protocol was performed twice to try to achieve the previous results.

The old protocol siRNA transfection was performed twice with infectivity following. The first run of knockdown (3/8/22) resulted in 31% SPTBN1 expression or 69% decrease expression (Fig. 20). The infectivity resulted in decrease of infection among all the virus dilutions (Fig. 23). The procedure was performed again to verify the results. The second time with the old knockdown protocol (3/27/22) resulted in 8% SPTBN1 expression or 92% knockdown of SPTBN1 (Fig. 20). This was similar to the highest knockdown achieved for the new protocol. The resulting infectivity had a decrease of infection with SPTBN1 knockdown with the $1/32^{nd}$ dilution and smaller (Fig. 24). The $1/2^{nd}$ dilution caused an extreme increase in HIV infection. The $1/4^{th}$, $1/8^{th}$, and $1/16^{th}$ dilutions had small increases in HIV infection (Fig. 24). With the decrease in HIV infectivity with SPTBN1 knockdown shown with the old siRNA transfection protocol, it was used for all other knockdown procedures.

Fusion Assay

Fusion kinetics were next investigated by adding a fusion inhibitor to infected cells overtime. These cells had SPTBN1 or NT siRNA transfection to see if SPTBN1 knockdown alters fusion. The NT siRNA should not target anywhere in the genome and therefore should not alter fusion but is a control for adding siRNA to the cells. To determine the proper fusion inhibitor, ammonium chloride (NH_4Cl), concentration to use, a fusion assay was performed with various concentrations (10 mM, 25 mM, 50 mM, and 100 mM). New ammonium chloride was filter sterilized and used at the varying concentrations. One sample used 25 mM concentration old ammonium chloride for comparison to the new NH_4Cl. The infection percent was determined with flow cytometry and shown as percent GFP+ cells. All concentrations of ammonium chloride

had infection rates less than 0.45% (Fig. 25). The no treatment sample had 46% infection. The 100 mM ammonium chloride sample had the lowest rate of infection, but lower cell counts. The 10 mM concentration sample was also very low infection at 0.15% and the cells tolerated the ammonium chloride better (Fig. 25). Therefore, 10 mM ammonium chloride was used for all other ammonium chloride fusion experiments.

With the concentration of ammonium chloride determined, a fusion assay was performed to determine the kinetics of fusion in CHME3 cells. Ammonium chloride media was added in at various times after infection (0 hour, 15, 30, 45 minutes, 1, 2, 3, and 4 hours) and infectivity was determined by flow cytometry. The line made by the data points had a big increase of infection within the first hour and lesser but steady increase in infection from 1 to 4 hours (Fig. 26). This result was similar to the fusion kinetics of other cell lines (84, 85).

With fusion kinetics determined in cells with no expression changes, a knockdown of SPTBN1 was done to see how it affects fusion. The knockdown percentage achieved was 86% decrease in SPTBN1 expression (Fig. 27). The fusion results showed that in the first half an hour, fusion kinetics for SPTBN1 and NT transfection cells had the same fusion rate. From the 1 hour to the 4-hour post infection time point, SPTBN1 knockdown had a decreased rate of HIV infection compared to NT (Fig. 28). The Infection rates for all of the conditions was above 50% which may be inaccurate due to the increased probability of two or more viruses infecting one cell. The infection percent desired is below 50%, so a new stock of CHME3 cells were thawed, and the experiment was performed again.

The new CHME3 cells were used in a fusion assay as done previously. New virus was used at a concentration of 1 microliter in 100 μL from a stock made by Emma Wise. The knockdown percentage was determined to be 94% decrease of SPTBN1 expression or 6%

expression (Fig. 27). The fusion kinetics showed that SPTBN1 had more fusion in the first 15 minutes of the assay and kinetics were the same at the 30-minute time point. From the 45-minute time point on, the SPTBN1 knockdown cells had a slightly lower infection rate compared to the NT transfected cells (Fig. 29).

The fusion assay procedure was done once more to confirm the results. The knockdown achieved from this experiment was 81% knockdown (Fig. 27). The fusion kinetics of SPTBN1 and NT were compared and exhibited the same fusion rate for the first 45 minutes. After 45 minutes, the NT fusion increased to above 25% infection before leveling off while SPTBN1 fusion leveled off at just above 20% infection (Fig. 30A). To make sure the lower overall infection of SPTBN1 knockdown cells was not causing the change between the samples, the values were normalized to the highest percentage of infection for the respective samples. This was graphed comparing SPTBN1 and NT samples with the normalized fusion curves being closer than the unnormalized values (Fig. 30B). SPTBN1 had a slightly lower infection at the 3-hour time point with all other times being close to the NT infection. The half-life of HIV fusion for the three experiments was calculated for statistical analysis.

Each experiment was normalized by setting the highest fusion to 100% (Fig. 30B). Using the normalized values for each experiment, the time where 50% of HIV had fused in the sample was determined as the half-life. The half-life from the 7-7-22 experiment was 9 minutes and 22 seconds for SPTBN1 and 11 minutes and 57 seconds for NT samples. The 9-2-22 fusion experiment found the half-life for SPTBN1 samples to be 13 minutes 45 seconds and NT was 22 minutes 55 second. The final experiment on 9-16-22 determined the half-life of SPTBN1 samples to be 25 minutes and 15 seconds and NT 25 minutes and 26 seconds (Table 6). From these three independent experiments, the average half-life of fusion in SPTBN1 knockdown cells

was 16 minutes and 7 seconds and the average half-life of fusion NT knockdown cells was 19 minutes and 10 seconds. The standard error was determined and along with the average time was used in a t-test calculation. The p-value was determined to be 0.648, meaning the average half-life values were not statistically different between siRNA knockdown and control cells.

Table 2. Comparison of qPCR from Two Supermixes

	SsoFast EvaGreen Supermix		iTaq Universal SYBR Green One-Step Kit	
Plasmid DNA Dilution	GAPDH Primers C_q Average	SPTBN1 Primers C_q Average	GAPDH Primers C_q Average	SPTBN1 Primers C_q Average
10^5	24.40	23.81	21.60	21.01
10^4	17.88	20.16	14.97	17.77
10^3	14.60	14.37	11.44	11.70
No DNA	38.67	34.80	38.98	36.90

Table 3. Initial SPTBN1 primer efficiency qPCR values

Plasmid DNA Dilution	Initial Run (11-29-2021) Cq Values	Second Run (11-30-2021) Cq Values
10^5	9.37	8.97
10^4	14.73	15.34
10^3	20.62	21.79
10^2	25.92	26.52
10^1	30.06	30.22
Primer Efficiency	0.55	0.53

Table 4. Final SPTBN1 primer efficiency Cq values

Plasmid DNA Dilution	(1-24-2022) Cq Values	(1-27-2022) Cq Values
10^5	9.85	11.03
10^4	12.49	14.51
10^3	16.14	18.52
10^2	20.28	23.44
10^1	24.80	27.44
Primer Efficiency	0.84	0.74

Table 5. GAPDH primer efficiency Cq values

Plasmid DNA Dilution	(1-24-2022) Cq Values	(1-27-2022) Cq Values
10^5	13.56	13.45
10^4	17.29	17.59
10^3	22.28	22.65
10^2	27.00	28.04
10^1	32.46	32.21
Primer Efficiency	0.62	0.62

Table 6. Half-life of HIV fusion

	Half-life of fusion (min)*		
Infection Date	SPTBN1	NT	SPTBN1 Knockdown
7-7-22	9:22”	11:57”	85.7%
9-2-22	13:45”	22:55”	93.8%
9-16-22	25:15”	25:26”	80.8%
Average Time	16:07”	19:10”	
Standard error	4.74	3.92	

*Data difference not statistically significant.

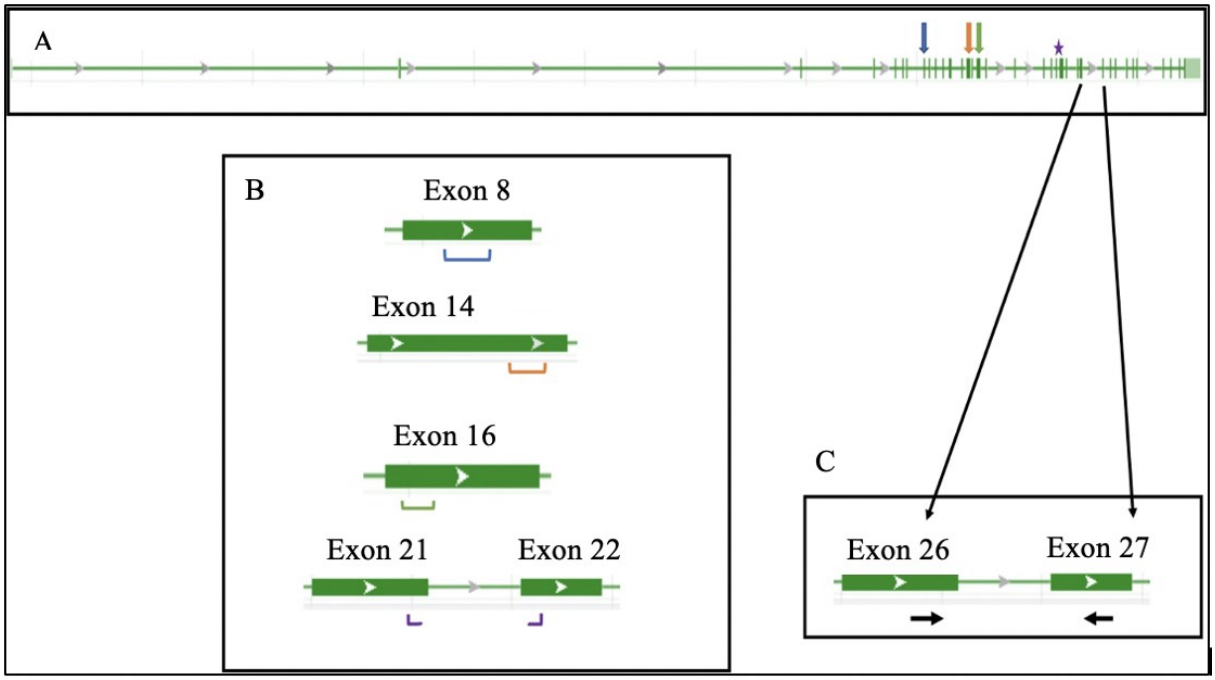

Figure 9. SPTBN1 Primer and siRNA Locations.
NCBI results of the SPTBN1 gene shows the introns and exons with the targets indicated. The exons are green vertical lines and introns are the horizontal lines connecting them for SPTBN1 (A). The siRNA target locations are shown along with the exon where the target recognizes with a bracket (B). Arrows and a star (spanning two exons) indicate where the target exons are in the entire gene. The forward and reverse primer sequences amplify within two exons shown by arrows with a larger image of where (C).

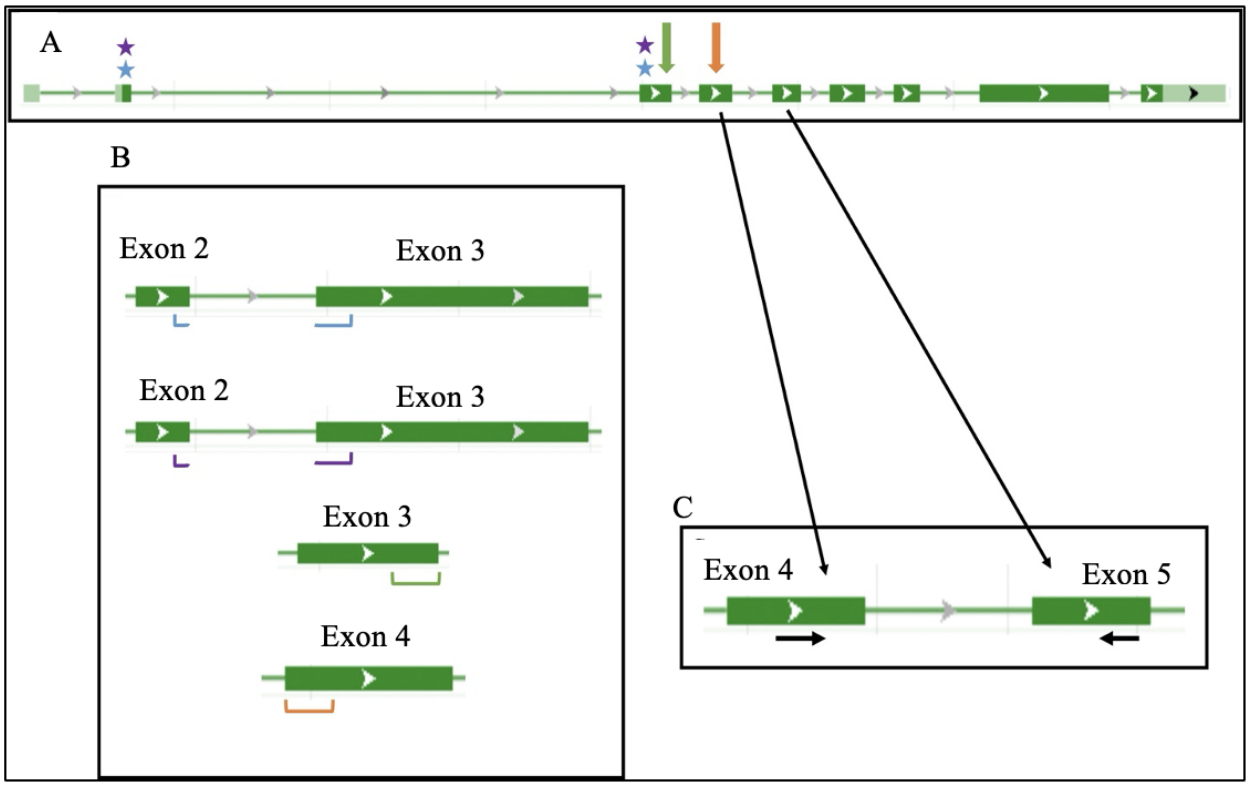

Figure 10. GAPDH Primer and siRNA Locations.
The GAPDH gene schematic was obtained through an NCBI search. The exons are thicker green boxes, and the introns are the lines between the exons (A). The siRNA target locations and exon number targeted are indicated by a bracket and color coordinated (B). Arrows and stars show the target exons in the entire sequence. The forward and reverse primer targets are enlarged with arrows showing the exon parts amplified (C).

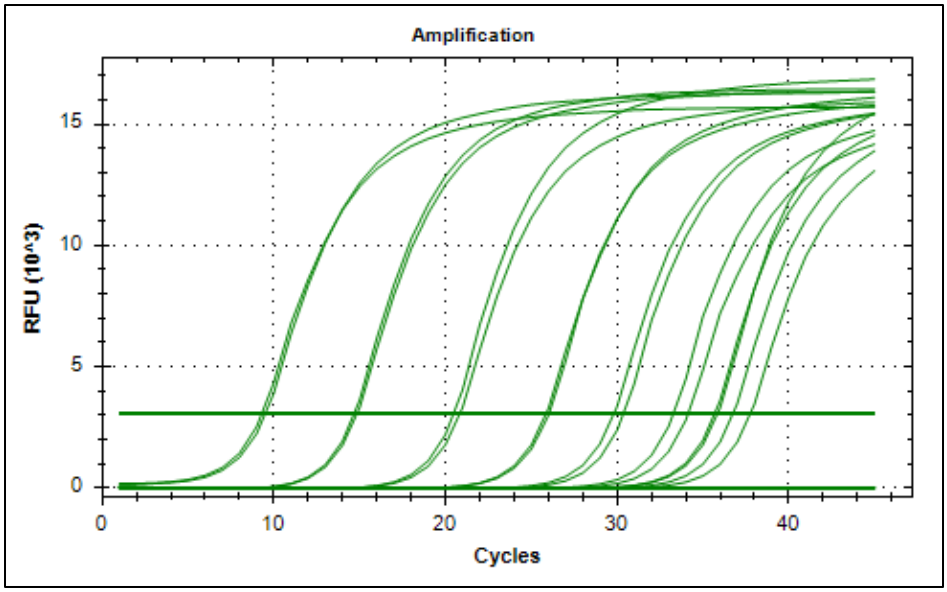

Figure 11. qPCR Amplification Curve.
The primer efficiency amplification curves from qPCR on 11-29-2021 with the SPTBN1 primers and the larger dilution volume. Relative fluorescence unit (RFU) indicates the level of fluorescence.

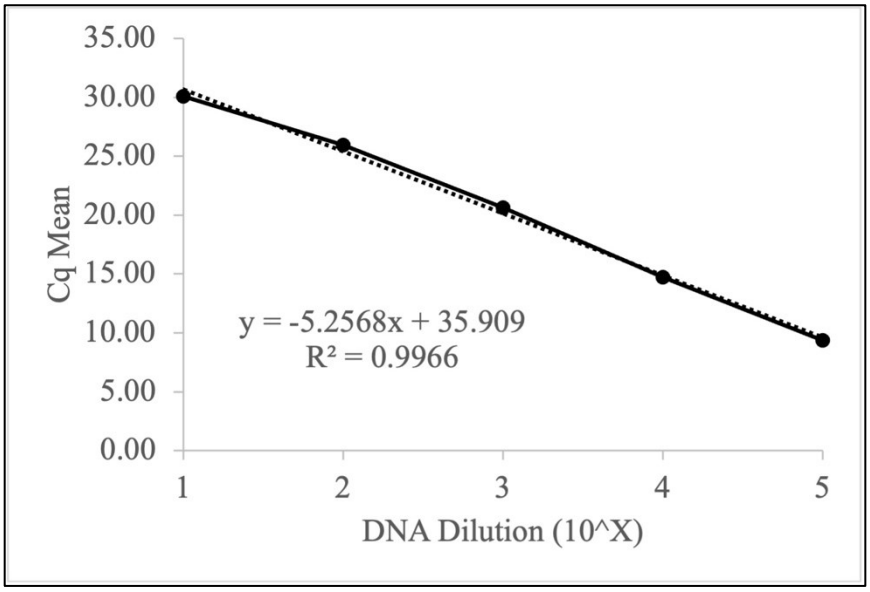

Figure 12. Standard Curve for 11-29-2021 qPCR Primer Efficiency.
A standard curve was made using the average C_q value of triplicate qPCR results from a serial dilution of plasmid DNA containing SPTBN1. The equation of the line and R-squared values for the data are present.

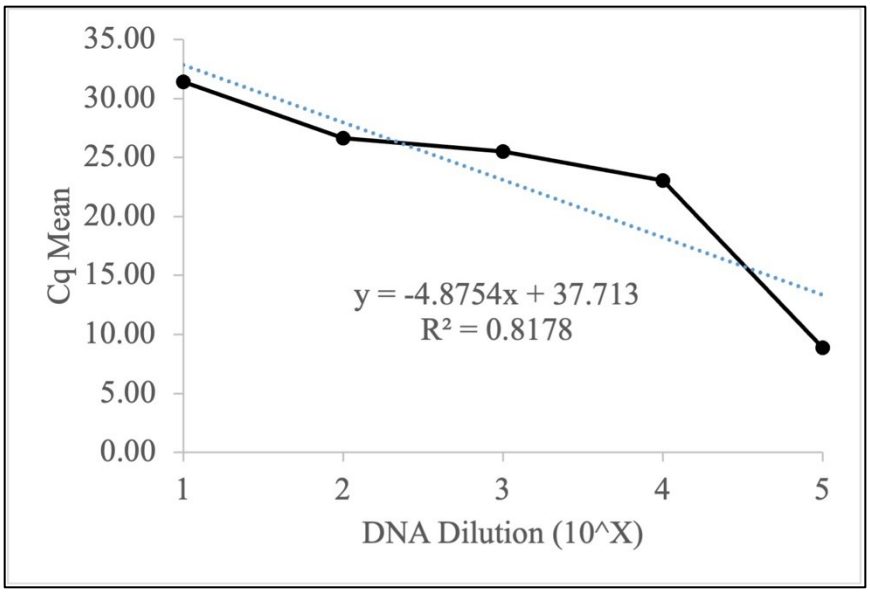

Figure 13. Standard Curve for 12-9-2021 qPCR SPTBN1 Primer Efficiency.
A standard curve was made using the C_q values of a serial dilution of plasmid DNA with the SPTBN1 gene present. The dilution was done in triplicate and the average values used as the data points.

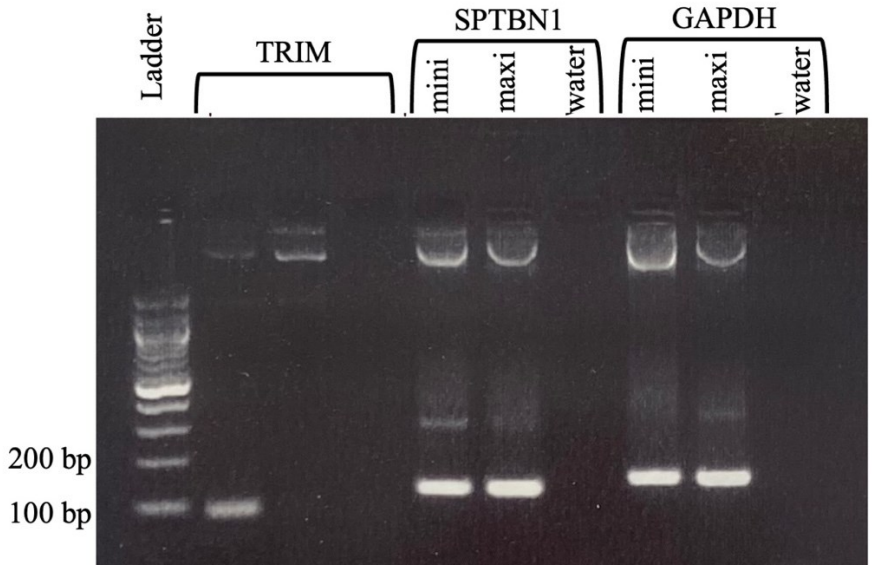

Figure 14. PCR Verification of Plasmid DNA.
PCR was performed on the Maxiprep isolated plasmid DNA with GAPDH or SPTBN1 genes present with the appropriate primers. The PCR samples were run on a gel to visualize the product sizes compared to a 100 bp ladder. TRIM was a sample separate from this thesis research. SPTBN1 expected size was 127 basepairs. GAPDH expected size was 151 basepairs.

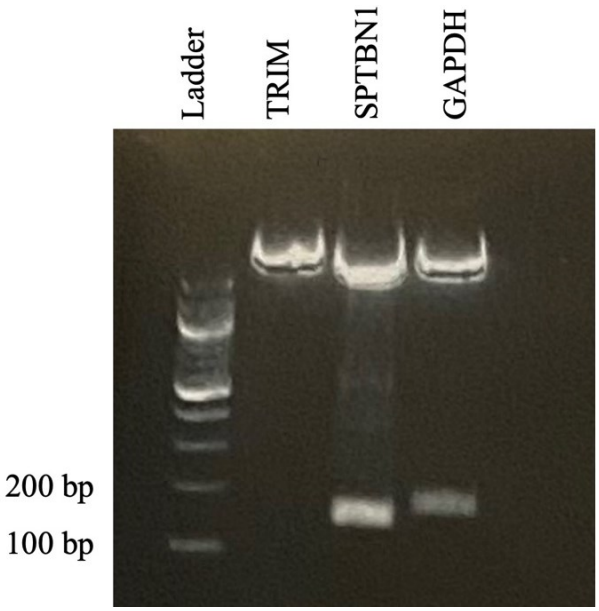

Figure 15. Restriction Digest Verification of Plasmid DNA.
The restriction digested newly isolated plasmid DNA with either GAPDH or SPTBN1 was ran on a gel to verify the product size. The product sizes were compared to a 100 bp ladder. TRIM was a sample separate from this thesis research. SPTBN1 expected size was 127 basepairs. GAPDH expected size was 151 basepairs.

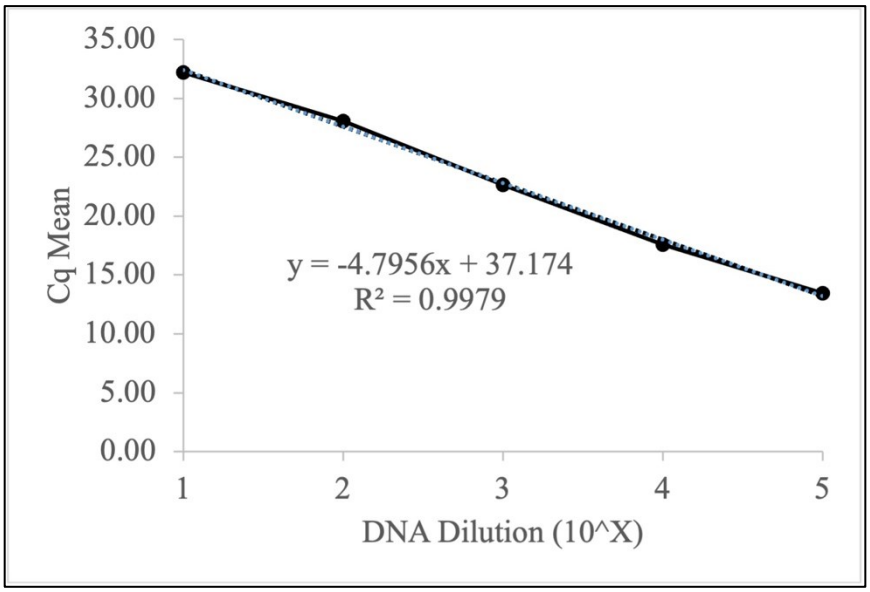

Figure 16. Standard Curve for 1-24-2022 GAPDH Primer Efficiency.
The Cq values from the 1-24-2022 GAPDH plasmid DNA serial dilution qPCR results were used for a standard curve. The R-squared value and equation of the trendline was present on the graph.

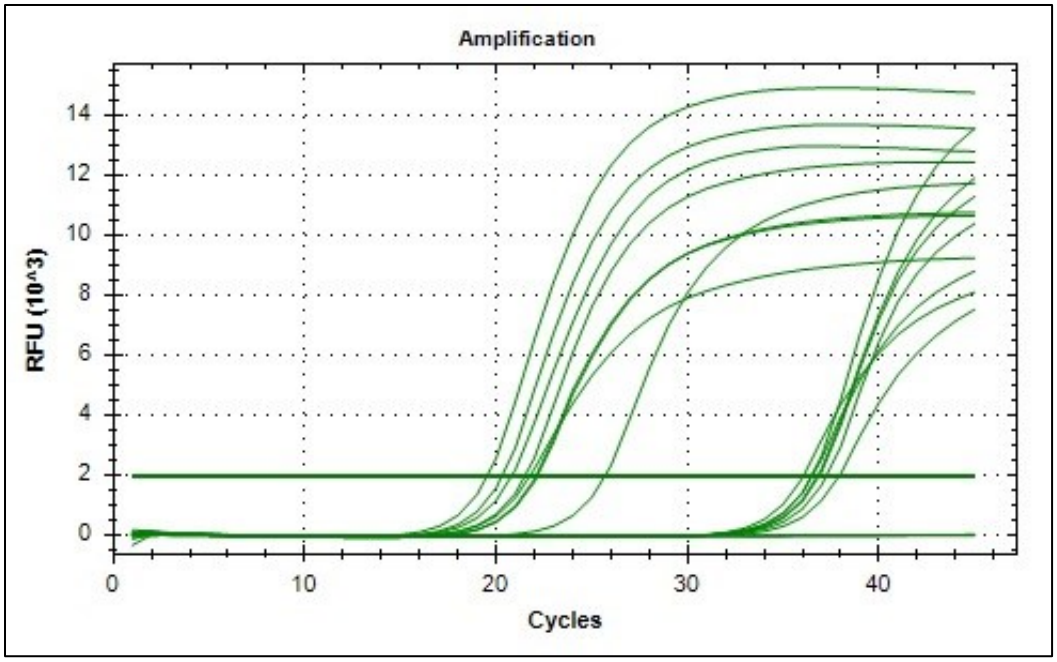

Figure 17. qRT-PCR Curves from SPTBN1 Knockdown.
RNA samples isolated from CHME3 cells that were transfected with SPTBN1 siRNAs based on two protocols. The qRT-PCR was performed to quantify the RNA levels using SPTBN1 and GAPDH primers. Relative fluorescence unit (RFU) indicates the level of fluorescence.

Normalized Fold Change = $(E_{p\text{-target}})^{\Delta CT\text{-target}} / (E_{p\text{-housekeeping}})^{\Delta CT\text{-housekeeping}}$

New Protocol Knockdown Calculation:

SPTBN1 (Target)	GAPDH (housekeeping)
$\Delta C_T = 22.09\text{-}25.69 = -3.6$	$\Delta C_T = 15.20\text{-}15.07 = 0.13$
$E_p = 0.79+1 = 1.79$	$E_p = 0.62+1 = 1.62$
$1.79^{-3.6} = 0.123$	$1.62^{0.13} = 1.065$

Normalized Fold Change

$0.123/1.065 = 0.115$

Old Protocol Knockdown Calculation:

SPTBN1 (Target)	GAPDH (housekeeping)
$\Delta C_T = 20.31\text{-}20.81 = -0.5$	$\Delta C_T = 15.40\text{-}15.63 = -0.23$
$E_p = 0.79+1 = 1.79$	$E_p = 0.62+1 = 1.62$
$1.79^{-0.5} = 0.747$	$1.62^{-0.23} = 0.895$

Normalized Fold Change

$0.747/0.895 = 0.835$

Figure 18. SPTBN1 Knockdown Calculations.
The Pfaffl method was used to determine the expression of SPTBN1 normalized to the housekeeping gene GAPDH. The Pfaffl efficiency (E_p) was taken to the power of the change in cycle number (ΔC_T) that the RNA product was amplified by qRT-PCR.

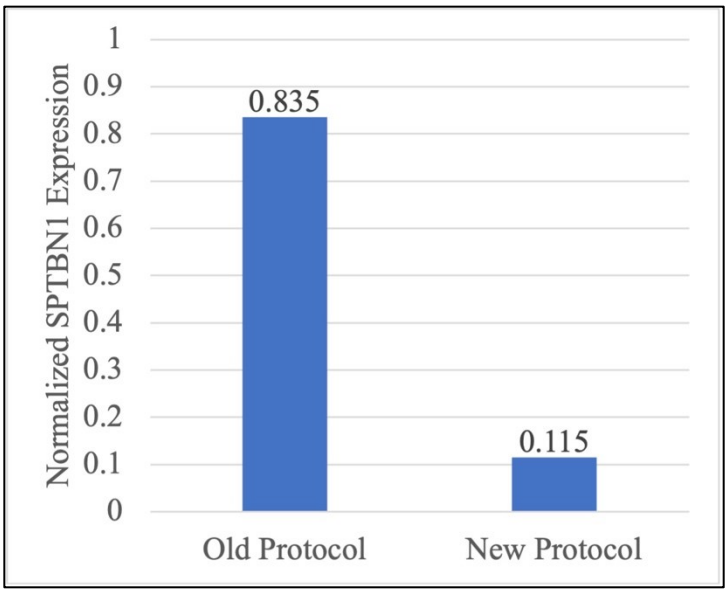

Figure 19. Comparing the Effectiveness of Two siRNA Knockdown Protocols.
The expression levels of SPTBN1 were quantified by qRT-PCR and calculated using the Pfaffl method. The knockdown of two protocols was compared with the expression shown as a decimal.

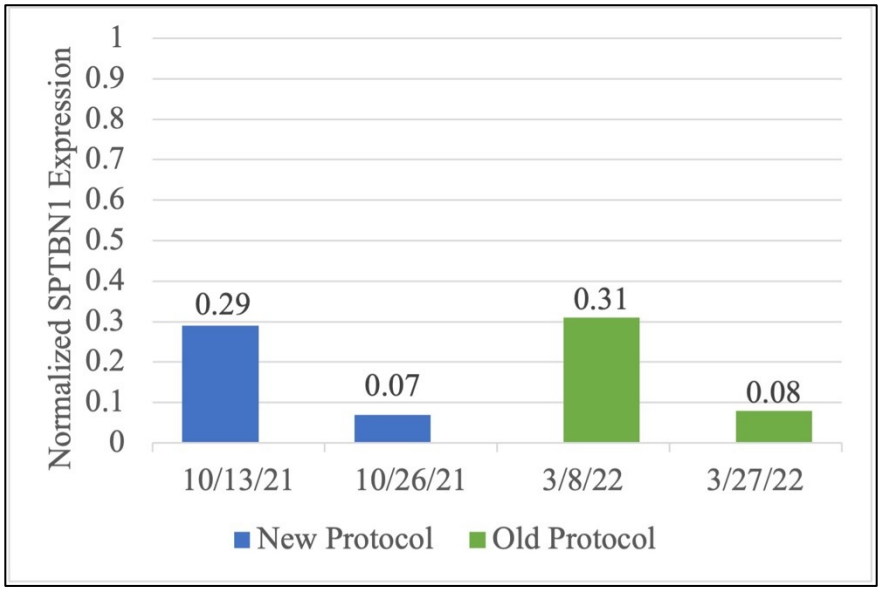

Figure 20. SPTBN1 Expression After siRNA Knockdown.
Two siRNA knockdown procedures were used to decrease SPTBN1 expression. The blue bars were the new knockdown protocol runs and the green were the old knockdown protocol runs. The expression of SPTBN1 was calculated as previously described in the Pfaffl method.

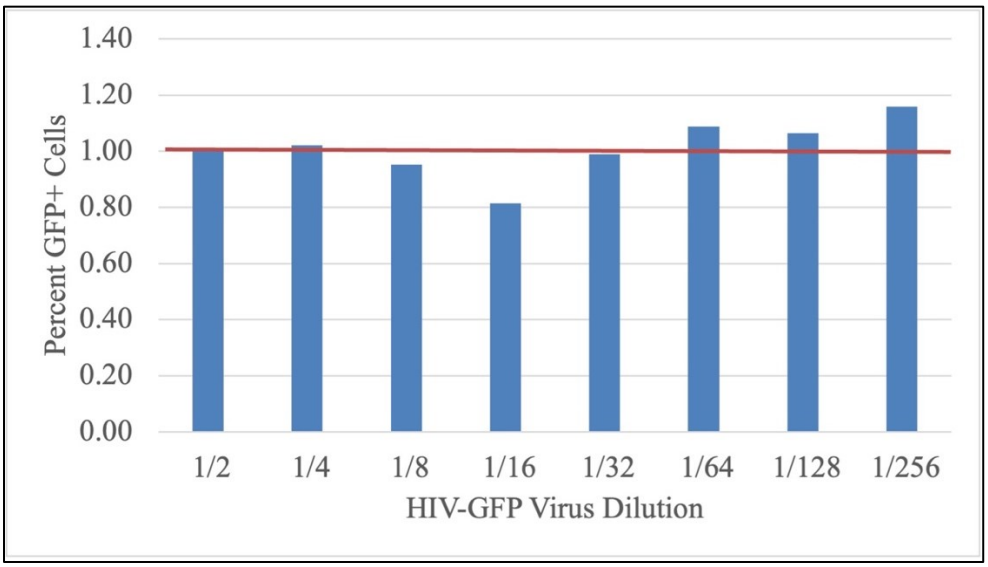

Figure 21. HIV Infectivity after SPTBN1 Knockdown 10-13-22.
With the new siRNA knockdown protocol on 10-13-22, CHME3 cells were then infected with HIV with a GFP reporter. The percent of cells infected was determined by flow cytometry and shown as percent GFP+ cells. Infection was normalized to the non-targeting knockdown samples at 1, shown with a red line. The no virus controls for SPTBN1 and NT were 0.12% and 0.08% respectively.

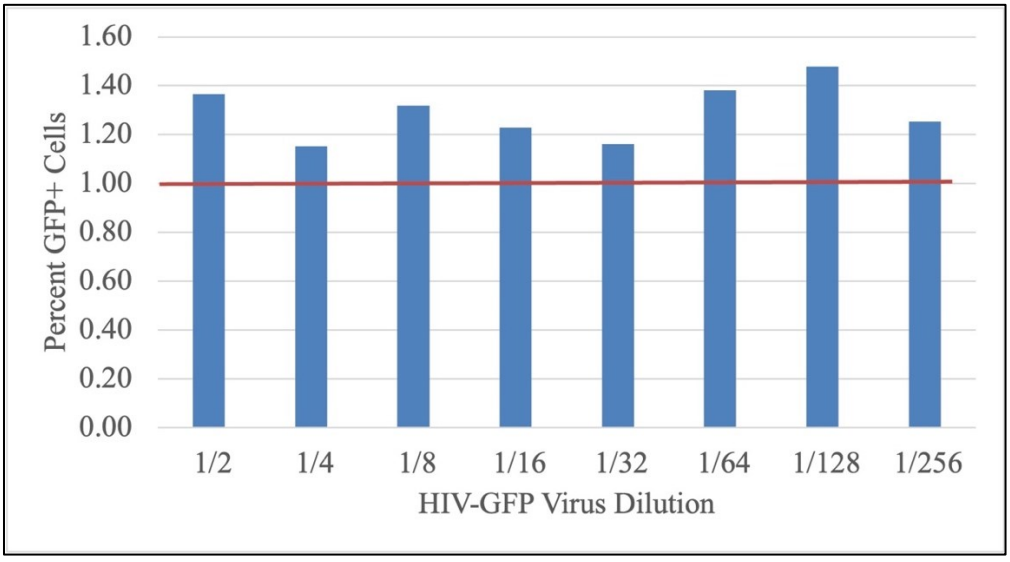

Figure 22. HIV Infectivity with SPTBN1 Knockdown 10-26-22 Experiment.
A second run of the siRNA knockdown new protocol was done with GFP reporter HIV infection. The infectivity indicated as GFP+ cells, was compared to the non-targeting siRNA transfection at 1 shown by a red line. The no virus controls for SPTBN1 and NT were 0.12% and 0.07% respectively.

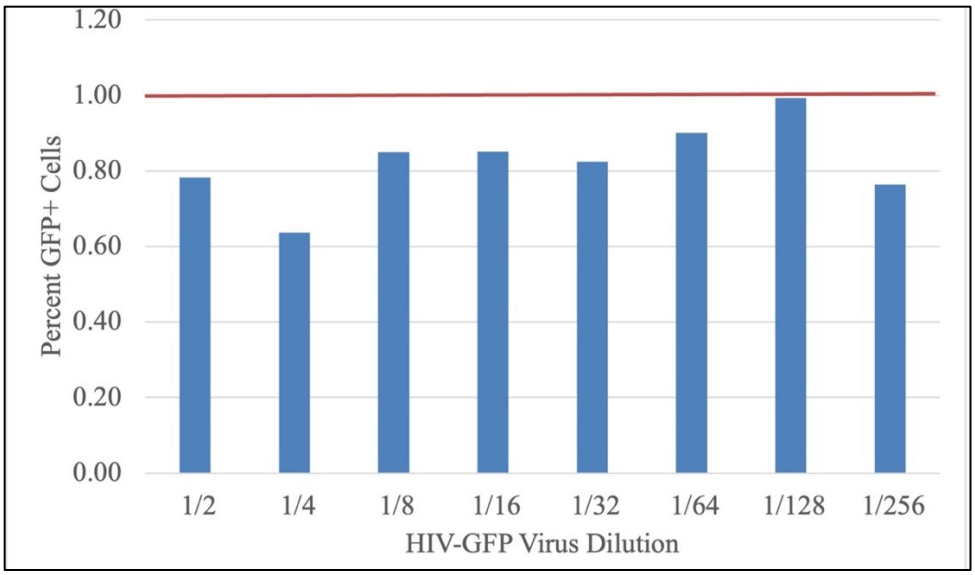

Figure 23. HIV Infectivity after SPTBN1 siRNA Knockdown 3-8-22.
The old siRNA knockdown protocol was used, and the cells were infected with HIV-GFP. Infectivity was determined by flow cytometry as GFP+ cells and normalized to the non-targeting siRNA transfection at 1 shown with a red line. The no virus controls for SPTBN1 and NT were 0.08% and 0.06% respectively.

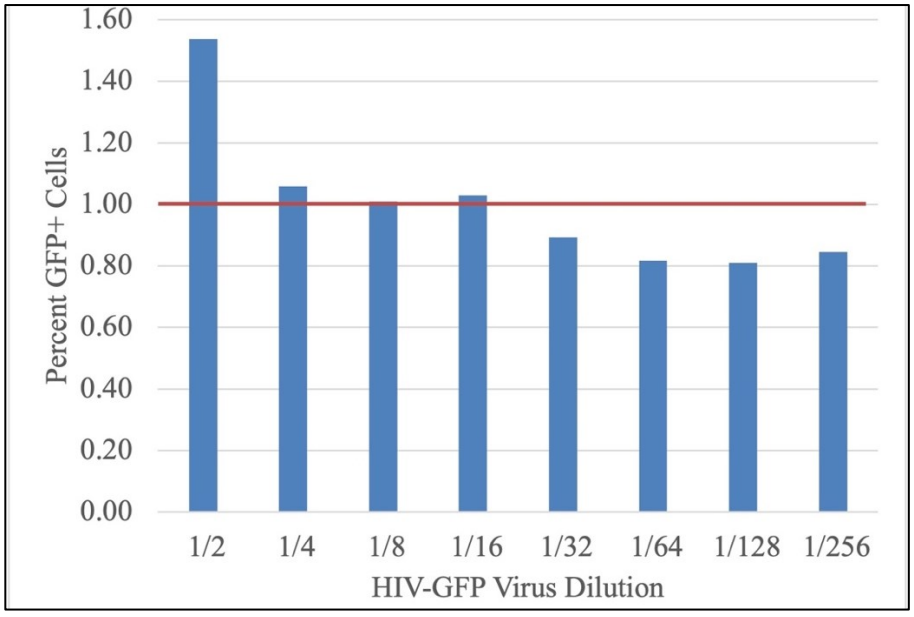

Figure 24. HIV Infectivity with SPTBN1 siRNA Knockdown 3-27-22.
Cells were infected with HIV-GFP after SPTBN1 knockdown using the old protocol. Infectivity was represented as GFP+ cells determined by flow cytometry. The percent infection was normalized to the non-targeting knockdown transfection at 1 shown by a red line. The no virus controls for SPTBN1 and NT were 0.05% and 0.08% respectively.

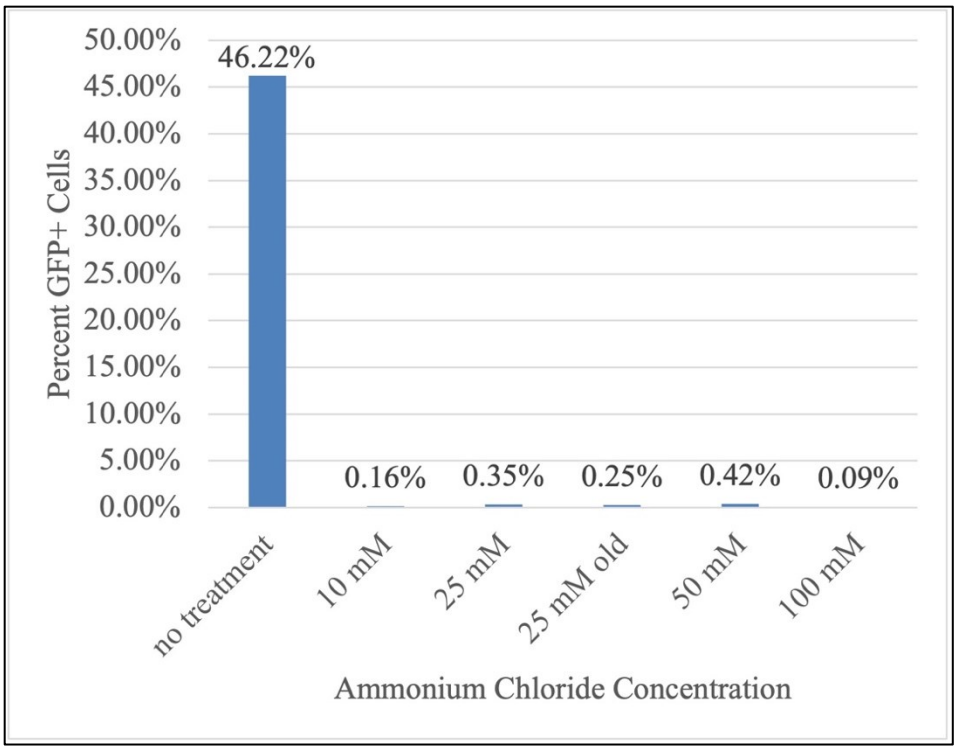

Figure 25. HIV Fusion Assay with Various Ammonium Chloride Concentrations.
A fusion assay was done with adding in different concentrations of ammonium chloride. The infectivity was determined by flow cytometry and was shown as percent GFP+ cells.

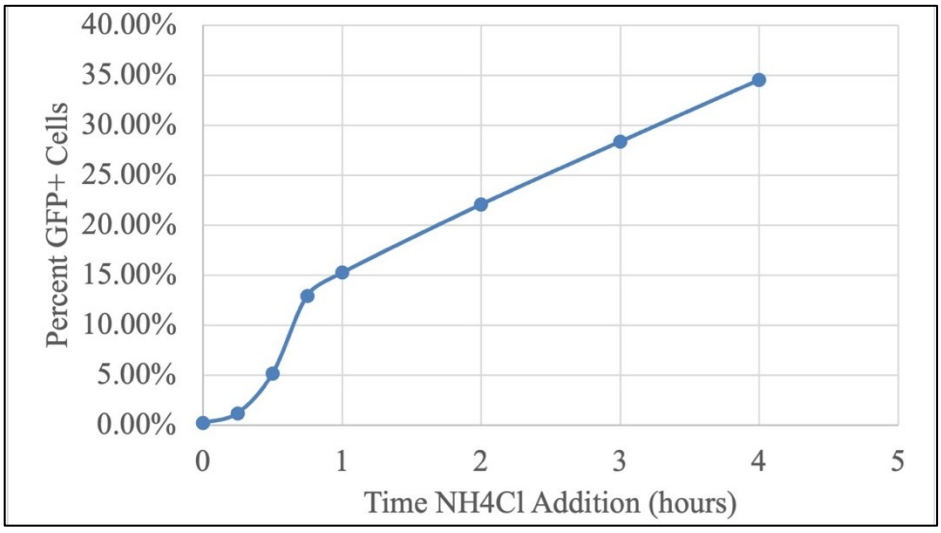

Figure 26. Fusion Kinetics Overtime.
A fusion assay was performed with 10 mM ammonium chloride added into cells infected with HIV. The add in was done over time and infectivity determined by flow cytometry shown as percent GFP+ cells.

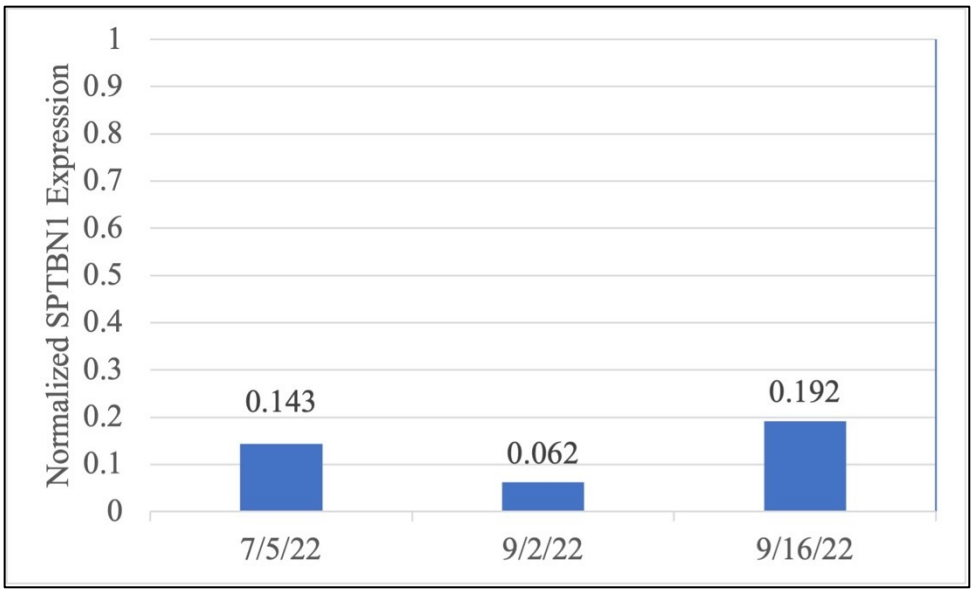

Figure 27. Expression of SPTBN1 after Knockdown for Fusion Assays.
For each fusion assay, the knockdown percentage of SPTBN1 was determined. The Pfaffl method was used to find the expression change from qPCR results compared to the non-targeting transfected samples with GAPDH as the housekeeping control.

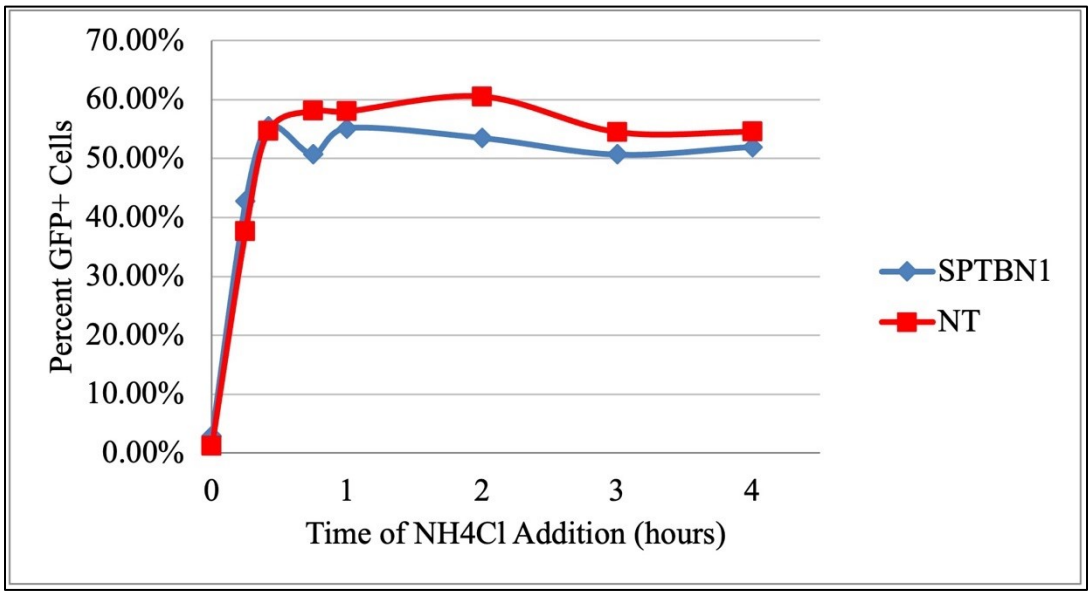

Figure 28. HIV Fusion Kinetics After siRNA Knockdown 7-7-22.
CHME3 cells were transfected with SPTBN1, NT, or no siRNA and a fusion assay was performed by adding NH_4Cl at various time points after infection (n=2). Percent GFP+ cells were determined by flow cytometry to indicate the HIV infection rate for each sample. The infectivity of SPTBN1 knockdown cells is the blue diamonds and the NT is red squares.

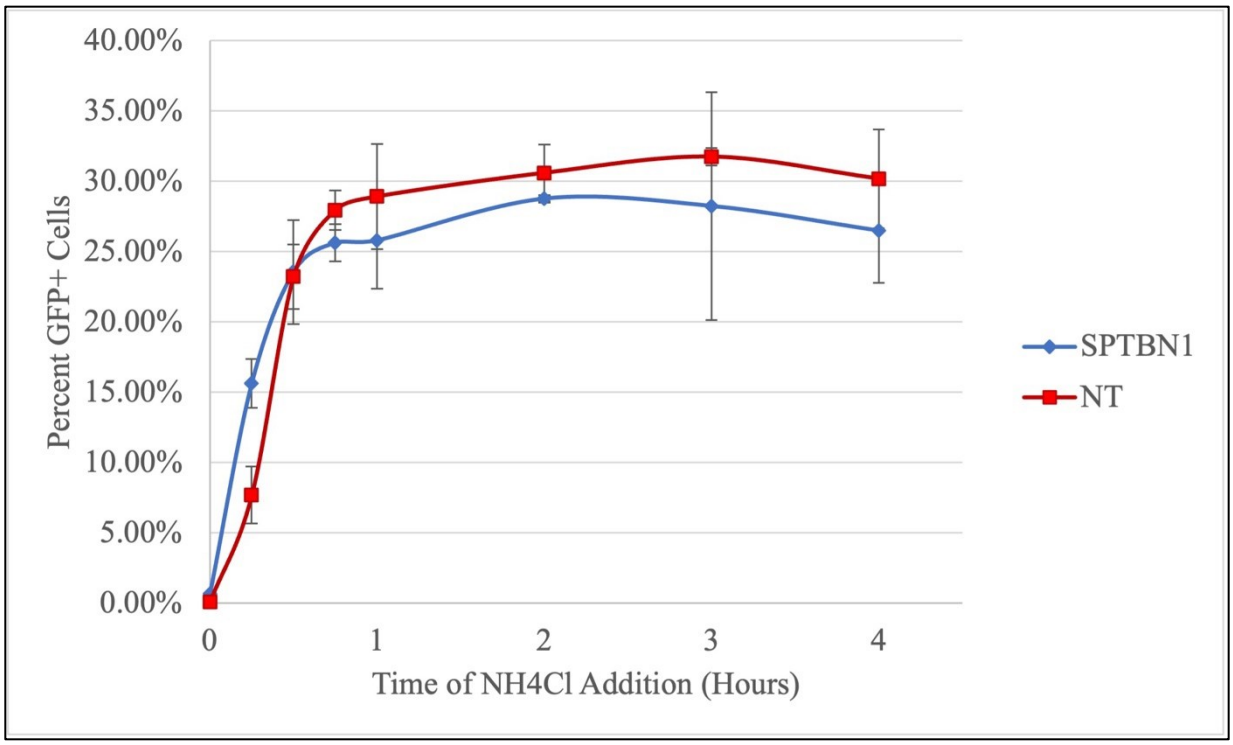

Figure 29. HIV Fusion Kinetics following SPTBN1 Knockdown 9-2-22.
Cells were transfected with SPTBN1 or NT siRNAs, infected with HIV-GFP, and a fusion inhibitor was added overtime to determine the fusion kinetics (n=3). Error bars indicate the standard deviation from the triplicate reactions. Flow cytometry was done to determine the number of cells that expressed GFP that indicates infection. The fusion of SPTBN1 is shown by the blue diamonds and NT is indicated by red squares.

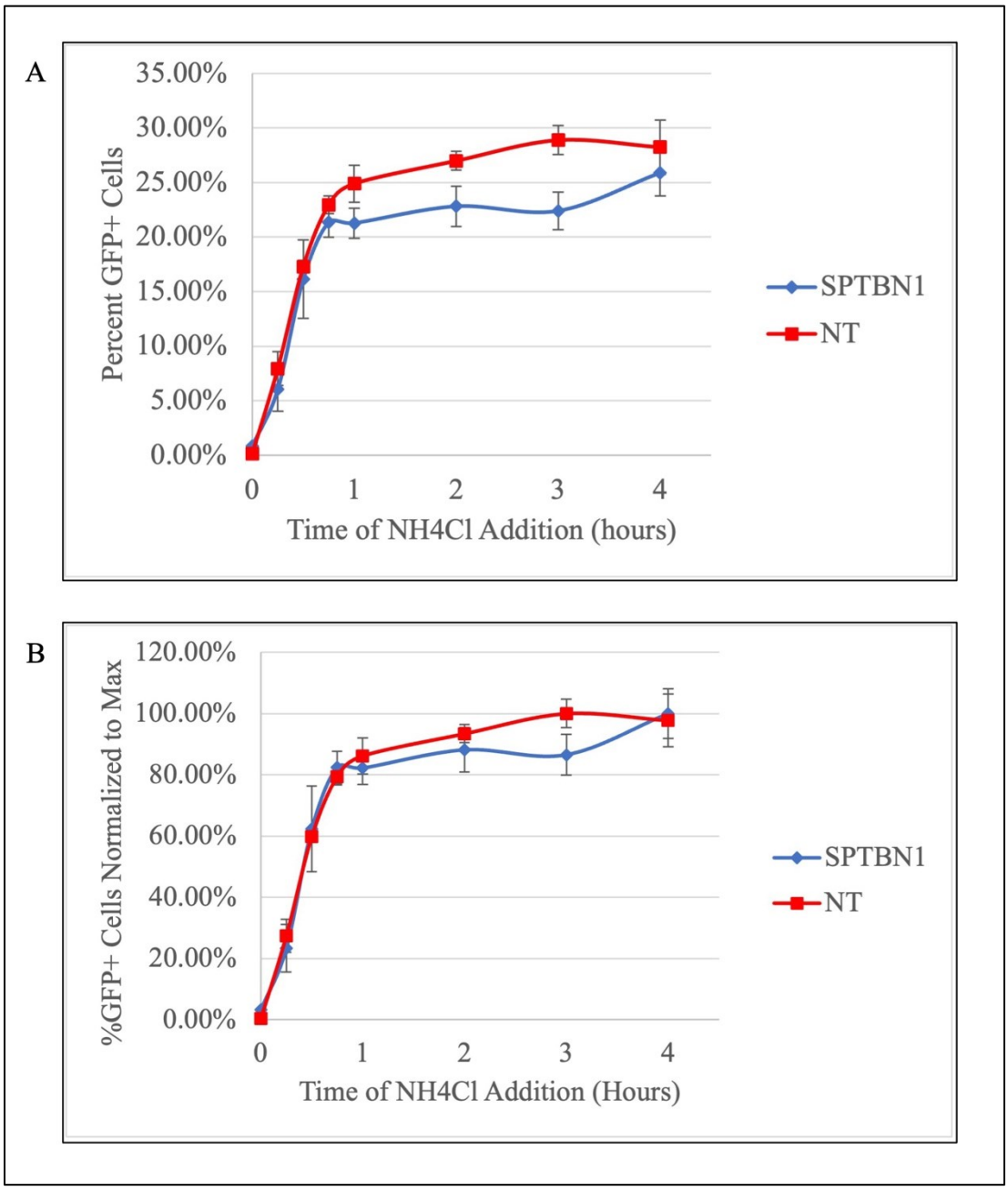

Figure 30. Fusion Assay After SPTBN1 Knockdown 9-16-22.
Microglial cells were transfected with SPTBN1, NT, or no siRNA before HIV infection. Following infection, the fusion inhibitor NH_4Cl was added in overtime to determine the fusion kinetics (n=3). Error bars indicate the standard deviation from the triplicate reactions. Infection percentage was determined by flow cytometry. SPTBN1 (blue diamonds) and NT (red square) siRNA transfected samples were compared on the percent of HIV infection (A). The values were normalized to the highest percent infection of that sample (B).

DISCUSSION

Bioinformatics was performed to ensure the targets of qPCR primers and siRNAs were in ideal locations and unique to the gene in question. The qPCR primers should be in different exons with an intron in the middle to ensure the primers are amplifying mature RNA or cDNA. The product size should not be too small that the polymerase cannot amplify the sequence and a product of 200 basepairs or less is ideal for qPCR to have the best primer efficiency (86). The siRNA locations should be in exons spanning the gene to maximize the knockdown. Both qPCR primers and siRNAs are only present in and affect the SPTBN1 or GAPDH genes. The qPCR forward and reverse primers for SPTBN1 and GAPDH are in exons with an intron in the middle (Fig. 9 and 10). The primers amplify a sequence between 100 and 200 basepairs long (Fig. 14 and 15). The siRNAs used were a mixture of 4 sequences that target different locations in the genes. Both SPTBN1 and GAPDH siRNAs targeted exons or spanned exons throughout the genes (Fig. 9 and 10). The qPCR primers and siRNAs used in this research meet all of the ideal characteristics based on the bioinformatics.

There are many qPCR protocols available that can be used depending on what samples are being tested. The optimization of the qRT-PCR protocol was performed as it is used to determine the knockdown expression level of SPTBN1. Two protocols were compared to see which one would have earlier amplification (a smaller C_q) and decreased background (larger C_q in the negative control). The new qRT-PCR protocol had the reverse transcriptase step included which is an advantage, making the protocol easier to use and decreasing the probability for contamination. With the same DNA samples and primers, the iTaq One-Step Kit had earlier amplification of the targets (GAPDH and SPTBN1) along with less background (Table 2). Earlier sample dection and less background is likely due to the polymerase. The taq polymerase

is a hot-start polymerase that requires high temperatures to activate the polymerase (87). This heat activation allows for reduced off target amplification and decreased primer dimers that cause greater background. The BioRad information for SsoFast also shows it having a lower specificity that could cause off target amplifcation resulting in slower detection and increased background (88). With the qRT-PCR protocol changed, the primer efficiency was recalculated with the iTaq supermix.

The SsoFast primer efficiency for SPTBN1 and GAPDH primers was determined by Marc Havlicek with SPTBN1 being 1.05 and GAPDH being 0.79 (75). Starting with the SPTBN1 primer set and using the iTaq one-step kit, the initial results had a much lower efficiency of 0.55. Low efficiency is not desired because it would indicate that the supermix and primers are not efficiently amplifying the products and should not be used together. Because the primer efficiency was about half of the efficiency that was found with the SsoFast supermix, each component of the qPCR sample was tested and analyzed to try to increase the efficiency. The primers were rediluted and used at a higher concentration to ensure there was enough of the primers to amplify the products. This did not increase the efficiency so it was determined that was not the cause of the lower efficiency (Fig. 13). The plasmid DNA used intitally was what Marc Havlicek used and could have degraded in storage so it was grown and reisolated to determine if that was the cause of the lower efficiency.

The plasmid DNA used contained either the GAPDH or SPTBN1 genes. After the plasmid DNA was isolated again, confirmation of the genes presence was done (Fig. 14 and 15). Both genes were present in the respective samples. The primer efficiency of SPTBN1 was continued with the new plasmid DNA for the dilution series. The SPTBN1 primer efficiency was determined to be 0.79 which is closer to the SsoFast primer efficiency. The GAPDH primer

efficiency was determined as well with the new plasmid DNA and is 0.62. Both primer efficiencies with the iTaq supermix were lower than the SsoFast primer efficiency but that was expected based on the BioRad website. It shows that SsoFast supermixes have a higher efficiency than iTaq supermixes (89). This higher efficiency could be due to the additives present in the SsoFast supermix that allow for the polymerase to amplify the target efficiently. Because the supermixes are propriertorized, the exact composistion of the mix is not public knowledge. As experiments continue, it is important to try to optimize the qPCR protocol as new potentially better products become available. The supermixes may have contain polymerases that amplify hard targets better, it could contain different additives that increase efficiency, or other various changes could be more ideal for the samples being tested. With a change in the qPCR supermix, primer efficiency should be recalculated because the contents of the supermix will affect how well the primers amplify the product (Table 4 and 5). In future, it could help to quantify the plasmid DNA using a nanodrop and make a serial dilution based on the concentration of DNA. This would also verify that the dilution series is accurate, with each dilution being $1/10^{th}$ of the previous. This would prevent unnecessary troubleshooting from an experiment with low R-squared value on the standard curve.

Another protocol that was optimized was the siRNA knockdown protocol to try to achieve a higher knockdown of SPTBN1. Two protocols were compared, the difference being the concentration of siRNA, incubation times, the media used on the cells during transfection, and if a media change was done following transfection (Fig. 31). The highest knockdown of SPTBN1 previously achieved by Marc Havlicek was 38.7% (75). The Dai Lab achieved about 90% knockdown of SPTBN1 (56). Along with the knockdown, the cells in culture were observed throughout the process to see if there was a drastic difference in the cells appearance. The initial

knockdown comparison resulted in the new knockdown procedure decreasing SPTBN1 expression much more than the old knockdown protocol, similar to what was seen in the Dai Lab (Fig. 19). The cells used with the old transfection procedure appeared more stressed in culture. The new protocol used less siRNA which could indicate that the old protocol was using too much siRNA that overwhelmed the cells.

Using the new siRNA transfection protocol, the SPTBN1 knockdown cells were infected with virus (Fig. 21 and 22). Previous research indicates that SPTBN1 knockdown decreases HIV infection with Marc Havlicek seeing 38.7% decrease in SPTBN1 expression caused a 37.5% decrease of infection. The Dai study showed that when SPTBN1 expression is decreased about 90% it causes over a 90% decrease of HIV infection in macrophages. The decrease of SPTBN1 expression did not initially decrease HIV infection in this research (Fig. 21 and 22; (56, 68, 74)). After SPTBN1 knockdown using the new siRNA transfection protocol, HIV infection stayed the same or increased compared to NT controls (Fig. 21 and 22). This was an unexpected result and its possible that the protocol used was not compatible with these cells.

The old protocol was returned to, to replicate the results previously achieved. There was one slight change to the transfection protocol that Marc Havlicek used. The final step is to add DMEM without penicillin-streptomycin (PS) to the minimal media already in the well, but in this research the media was changed completely to DMEM without PS (Fig. 31). The knockdown achieved after returning to the old transfection protocol was equivalent to the new protocol knockdown. It is likely that the slight change in the transfection protocol is the reason greater knockdown is achieved with the old protocol. It is easier on the cells when removing the media that contains the siRNAs and transfection reagent. Many siRNA transfection procedures have a media change to remove the transfection media (56, 90). The OPTIMEM media used in the

transfection protocols is a reduced serum media that starves the cells as they are being transfected. When cells are starved of nutrients, they are more willing to take in things in their environment such as siRNAs. The media change in the altered old transfection protocol brings back the nutrients the cells need and removes the harsh transfection reagent.

Going back to the old siRNA knockdown protocol generated the expected results of SPTBN1 knockdown decreasing HIV infection at lower virus concentrations (Fig. 23 and 24). In one experiment with the old transfection protocol, at higher virus concentrations, there was an increase in infection (Fig. 24). It is possible that there is a threshold of virus that the CHME3 knockdown cells can handle and with high SPTBN1 knockdown and high virus concentration, the cells become overwhelmed and more susceptible to HIV infection. The Dai study did show a high knockdown level having equally as high decrease of infection within macrophages (56). The cells used in this research are microglial cells that are a specialized macrophage in the central nervous system that could have a different reaction to SPTBN1 knockdown and HIV infection (91). Microglial cells have a drastically different gene expression profile than macrophages in the brain and would cause the difference during HIV infection (91). SPTBN1 is required for the cells and stabilizes the cytoskeleton. The cytoskeleton is altered significantly in macrophages with actin knockdown, shown by the Dai Lab, which causes stress on the cells (56). Adding a high concentration of HIV to the already stressed cells could overwhelm them and result in an increased rated of HIV infection.

To investigate this relationship further, it would be useful to vary the amount of SPTBN1 knockdown and see the change in HIV infection. Changing the concentration of siRNA in transfection would be a good start to lessen the amount of knockdown. With a drastically smaller concentration of siRNA, there wouldn't be enough available to completely knockdown SPTBN1

in every cell, but it may provide slightly decreased expression in all the cells. A dilution series of siRNA concentrations could be tested to see if the knockdown amount can be strategically achieved. If the siRNA knockdown can be less severe, the infectivity would then be tested to see if there is a correlation in the knockdown percentage to the decrease of HIV infection. From Marc Havlicek and the Dai study it seems there is the same decrease of HIV infection as SPTBN1 knockdown. This research did not generate the results the Dai study did where 90% knockdown caused a 90% decrease of infection (56). In this research when the knockdown of SPTBN1 was 80-90% the infectivity decreased consistently around 20% (Fig. 23, 24, and 30B). This again could be due to the microglial cells being overwhelmed with the siRNA knockdown and not having the same level of effect on infectivity. The Dai study did use a decreased amount of siRNA at 50 μM and had a media change following transfection (56). It is possible the siRNA concentration is too high in the old transfection protocol and causing more off target problems when HIV it trying to infect the cells. Further adjustments to the siRNA protocol should be done to see how that changes HIV-1 infection.

Troubleshooting the siRNA protocol could start with using the RNAiMAX transfection protocol but using the media the old transfection protocol used (Fig. 31). If the cells have the OPTIMEM media during transfection and a media change after transfection but everything else as in the RNAiMAX protocol it could be a starting point to what parts of the protocol are causing the increased knockdown. I would start by changing one step in the protocol at a time and continue from there, looking at the siRNA concentration, media present on the cells, and incubation times to further optimize the protocol.

The confirmation of SPTBN1 playing a role in HIV infection led to the question of what step in the infection process is it involved. Marc Havlicek found that SPTBN1 knockdown

altered uncoating kinetics (75). Because fusion is prior to uncoating, it is important to verify that fusion delay was not the reason uncoating was delayed. Therefore, Aim 2 of this thesis research determined whether HIV fusion kinetics was altered after SPTBN1 knockdown. It was hypothesized that SPTBN1 knockdown would affect HIV fusion kinetics in microglial cells. CHME3 cells without SPTBN1 knockdown have similar fusion to many other cell types (Fig. 26; (84, 85)). The fusion kinetics after SPTBN1 knockdown were compared to the NT control to see if there was a change. The half-life of fusion with SPTBN1 and NT transfected cells was calculated, and statistical analysis performed by an independent t-test. The SPTBN1 knockdown did not affect fusion of HIV (Fig. 28-30; Table 6). The half-life of HIV fusion for SPTBN1 knockdown was 16 minutes and 7 seconds, the NT was 19 minutes and 10 seconds (Table 6). These half-life times are not statistically different from each other ($p=0.648$). SPTBN1 knockdown decreases overall infection and is observed in the fusion experiments with lower percentages of infected cells compared to the NT (Fig. 28-30). When the experiments are normalized to the maximum amount of infection, the fusion rate is the same (Fig. 30). This indicates that the SPTBN1 is not involved in HIV-1 fusion, disagreeing with the hypothesis that SPTBN1 is involved in fusion.

SPTBN1 is an actin associated molecule, and actin localization occurs when HIV is infecting a cell during the fusion step specifically (66, 92). SPTBN1 organizes the actin cytoskeleton, without this present it affects the organization and in turn was thought to affect HIV infection steps that use actin (56). SPTBN1 is involved in HIV infection, but not the fusion step. This further supports the previous findings that SPTBN1 knockdown is involved in the uncoating of HIV. There are many future directions that could be performed to further investigate the role SPTBN1 has on HIV infection.

The aspirational Aim 3 of this research was not started due to time constraints and would be a future direction of research. The goal of the third aim is to visualize cytoskeletal elements of the cells and HIV via fluorescence microscopy to determine possible interactions and mechanisms of infection. The actin cytoskeleton will be visualized using phalloidin and SPTBN1 visualized by an antibody. There are many experimentation routes that can be taken with these methods. First the actin and SPTBN1 should be visualized before and after SPTBN1 knockdown. Before SPTBN1 knockdown, the actin would be a network throughout the cell with SPTBN1 organizing the filaments (56, 71). The actin cytoskeleton with SPTBN1 knockdown would be greatly affected, creating localized spotting rather than a fluid network (56). The presence of SPTBN1 should be decreased almost to nonexistent expression. The SPTBN1 location can also be visualized in relation to HIV virions using dual labeled virus. The dual labeled virus is pseudotyped with VSV-g envelope and two fluorescent markers within it; the GFP reporter on the Vpr viral molecule to signify the viral genome and a dTomato or mCherry label bound to the viral membrane. Dual labeled virus, like all virus used in this research enters the cell through endocytosis which is different than the fusion of wildtype HIV. The membrane marker of the dual labeled virus allows for differentiating virus with and without the membrane or virus that has entered the cytoplasm or not. This would verify that SPTBN1 is not involved in the fusion step of HIV, expecting the virions with the membrane intact would not colocalize with SPTBN1, but SPTBN1 should be colocalized somewhere after fusion. The SPTBN1 protein has been shown to interact with capsid and matrix viral proteins (56). Understanding at what point and how significantly these viral proteins interact with SPTBN1 is another step in understanding the mechanism of HIV infection. This could also be observed after SPTBN1 knockdown to see how

the route of HIV infection is altered. Because it is not likely that SPTBN1 is involved in fusion, the uncoating of HIV should be looked at again.

Identifying in what way SPTBN1 interacts with the capsid would further verify that the uncoating step uses actin and associated molecules to be complete. Marc Havlicek found that uncoating is delayed with SPTBN1 knockdown. The knockdown Marc achieved was 38.7%, much lower than what is now being achieved. It is important to go back and rerun the uncoating assays with higher SPTBN1 knockdown to verify that SPTBN1 is still being affected. This could also indicate if higher SPTBN1 knockdown decreases uncoating at the same or a different rate. An additional area to look at would be doing fluorescence microscopy but focusing on the capsid. Using an antibody for SPTBN1 and the HIV capsid would show if there is an interaction between the two molecules during infection. SPTBN1 has been shown to interact with the capsid and matrix proteins through immunoprecipitation by the Dai Lab. Visualizing this interaction during infection is needed to verify SPTBN1 is directly involved in uncoating. The matrix protein is involved in early replication steps following virus entry including being necessary for effective uncoating and reverse transcription (93, 94). It would be expected that SPTBN1 antibody would colocalize with the capsid antibody after the capsid is released into the cytoplasm and before entry into the nucleus.

This leads to the question of what other early infection processes involve SPTBN1. The Dai Lab showed SPTBN1 interaction with the capsid and matrix proteins, but these two proteins are involved in more than uncoating (56, 94). Other early replication steps may also involve SPTBN1, such as trafficking, reverse transcription, and entry into the nucleus. The early steps of HIV have the capsid and matrix proteins associated and it is necessary to determine whether SPTBN1 only associates with the viral complex during certain steps or at multiple steps.

Trafficking towards the nucleus could be initially investigated during the microscopy experiments to see if SPTBN1 is associated with the viral core for a long time and distance. If it is shown that SPTBN1 is associated with the HIV core the majority of the time in the cytoplasm, it likely means it plays a role in reverse transcription as well. Uncoating and reverse transcription have a lot of interplay and are happening at the same time within the cell (31, 34, 35). The amount of reverse transcription occurring before and after SPTBN1 knockdown can be tested similarly to that of fusion, with a reverse transcription inhibitor being added over a time course. This would indicate if and at what point reverse transcription is affected by SPTBN1 knockdown. The possible involvement of SPTBN1 in viral entry into the nucleus could be observed using microscopy as well. DAPI staining the nucleus and observing colocalization of SPTBN1 and the viral core would indicate SPTBN1 is present as HIV is entering the nucleus. The actin cytoskeleton is involved in entry into the nucleus, so it would be expected that the scaffolding protein of actin, SPTBN1, would also be present during the HIV core entering the nucleus (65, 66, 95).

The goal of this thesis research was to determine the role of SPTBN1 in HIV-1 infection. It verified previous research that SPTBN1 knockdown decreased HIV-1 infection (56, 68, 74). SPTBN1 knockdown has an effect on HIV-1 uncoating, observed in Marc Havlicek's thesis research, and this research shows that it does not have an effect on HIV-1 fusion (75). Therefore, this supports the conclusion that SPTBN1 is involved with the uncoating step of HIV infection. Understanding the HIV-1 replication cycle is imperative to finding a possible mechanism for treatments and a cure for those living with HIV.

HIV has been shown to interact with many microtubule associated proteins, but interaction with an actin associated protein gives more insight to how HIV infects microglia

cells. Microglia cells are long lasting cells and the innate immune systems defense within the central nervous system (17). These cells protect the CNS from infection that can lead to severe neurological defects. HIV infection of microglial cells are a large portion of the HIV reservoir where the viral DNA lays dormant within cells. The HIV reservoir is the biggest battle when trying to treat and cure HIV infection because the cells are not actively producing virus but after each cell division the progeny also contain the viral DNA (17). Preventing initial HIV infection in all cells, microglial cells especially is a major goal of HIV research. If a block to HIV infecting a cell is determined, once someone is exposed, treatment can be given, and chronic HIV infection avoided. Much of HIV research is trying to better understand the infection process and what cellular factors are involved. Once the mechanisms of HIV infection are uncovered, treatments to block those processes can be formulated to decrease and eventually irradicate HIV.

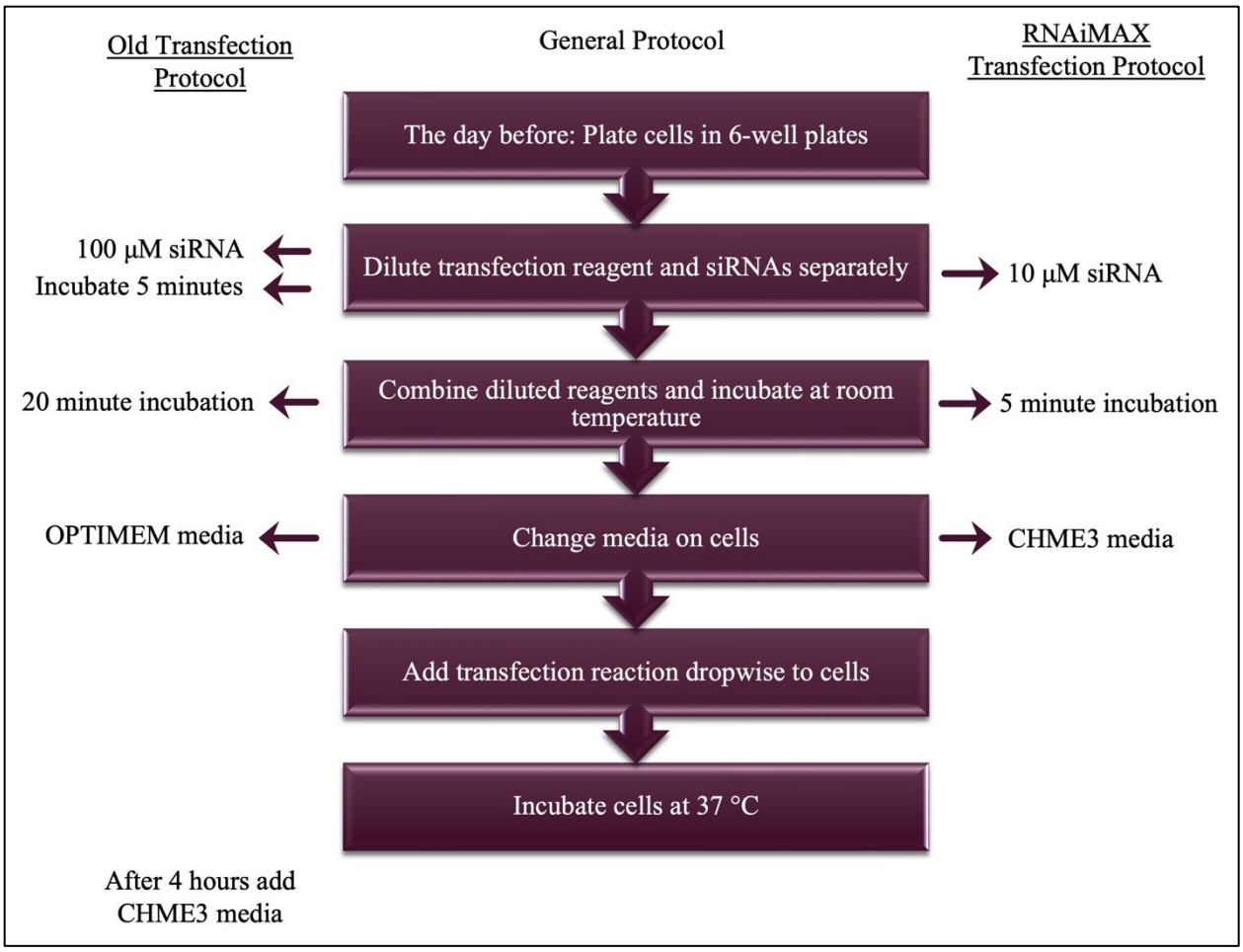

Figure 31. siRNA Transfection Protocol Comparison.
Two siRNA transfection protocols were compared to increase knockdown of SPTBN1. The general protocol stated in the diagram with arrows showing where the two protocols differ. The old transfection protocol was used by previous graduate students and the RNAiMAX transfection protocol comes with the reagents (80).

REFERENCES

1. 2021. HIV Basics. CDC. https://www.cdc.gov/hiv/basics/index.html. Retrieved 4 October 2021.

2. Global HIV & AIDS statistics — Fact sheet. UNAIDS. https://www.unaids.org/en/topic/data. Retrieved 4 October 2021.

3. **Nyamweya S, Hegedus A, Jaye A, Rowland-Jones S, Flanagan KL, Macallan DC.** 2013. Comparing HIV-1 and HIV-2 infection: Lessons for viral immunopathogenesis. Rev Med Virol 23:221–240.

4. **Taylor BS, Sobieszczyk ME, McCutchan FE, Hammer SM.** 2008. The challenge of HIV-1 subtype diversity. N Engl J Med 358:1590–1602.

5. **Peck KM, Lauring AS.** 2018. Complexities of viral mutation rates. J Virol 92.

6. **Mitra S, Shanmugapriya S, Santos da Silva E, Naghavi MH.** 2020. HIV-1 exploits CLASP2 to induce microtubule stabilization and facilitate virus trafficking to the nucleus. J Virol 94.

7. **Meriki HD, Tufon KA, Anong DN, Atanga PN, Anyangwe IA, Cho-Ngwa F, Nkuo-Akenji T.** 2019. Genetic diversity and antiretroviral resistance-associated mutation profile of treated and naive HIV-1 infected patients from the Northwest and Southwest regions of Cameroon. PLoS One 14:e0225575.

8. **Lee B, Sharron M, Montaner LJ, Weissman D, Doms RW.** 1999. Quantification of CD4, CCR5, and CXCR4 levels on lymphocyte subsets, dendritic cells, and differentially conditioned monocyte-derived macrophages. Proc Natl Acad Sci U S A 96:5215–5220.

9. **Tolbert WD, Sherburn R, Gohain N, Ding S, Flinko R, Orlandi C, Ray K, Finzi A, Lewis GK, Pazgier M.** 2020. Defining rules governing recognition and Fc-mediated effector functions to the HIV-1 co-receptor binding site. BMC Biol 18:91.

10. **Cooper A, García M, Petrovas C, Yamamoto T, Koup RA, Nabel GJ.** 2013. HIV-1 causes CD4 cell death through DNA-dependent protein kinase during viral integration. Nature 498:376–379.

11. **Battistini Garcia SA, Guzman N.** 2021. Acquired immune deficiency syndrome CD4+ countStatPearls. StatPearls Publishing, Treasure Island (FL).

12. **Manches O, Frleta D, Bhardwaj N.** 2014. Dendritic cells in progression and pathology of HIV infection. Trends Immunol 35:114–122.

13. **Storey M, Jordan S.** 2008. An overview of the immune system. Nurs Stand 23:47–56; quiz 58, 60.

14. **Alberts B, Johnson A, Lewis J, Raff M, Roberts K, Walter P.** 2002. Innate Immunity. Garland Science, London, England. Retrieved 11 April 2022.

15. 2020. The innate and adaptive immune systems. Institute for Quality and Efficiency in Health Care (IQWiG). Retrieved 11 April 2022.

16. Immune cells. National Institute of Allergy and Infectious Diseases. https://www.niaid.nih.gov/research/immune-cells. Retrieved 11 April 2022.

17. **Wallet C, De Rovere M, Van Assche J, Daouad F, De Wit S, Gautier V, Mallon PWG, Marcello A, Van Lint C, Rohr O, Schwartz C.** 2019. Microglial cells: The main HIV-1 reservoir in the brain. Front Cell Infect Microbiol 9.

18. **Abbas W, Tariq M, Iqbal M, Kumar A, Herbein G.** 2015. Eradication of HIV-1 from the macrophage reservoir: an uncertain goal? Viruses 7:1578–1598.

19. 2015. Homepage. https://www.hiv.gov/node/3641. Retrieved 4 October 2021.

20. **Arts EJ, Hazuda DJ.** 2012. HIV-1 antiretroviral drug therapy. Cold Spring Harb Perspect Med 2.

21. **Freed EO.** 2001. Somatic Cell Genet 26:13–33.

22. **Das AT, Harwig A, Berkhout B.** 2011. The HIV-1 Tat protein has a versatile role in activating viral transcription. J Virol 85:9506–9516.

23. German Advisory Committee Blood (Arbeitskreis Blut), Subgroup 'Assessment of Pathogens Transmissible by Blood.' 2016. Human immunodeficiency virus (HIV). Transfus Med Hemother 43:203–222.

24. **Medina-Trillo C, Sedgwick DM, Herrera L, Beltrán M, Moreno Á, Barrio P, Bedoya LM, Alcamí J, Fustero S, Gallego J.** 2020. Nucleic acid recognition and antiviral activity of 1,4-substituted terphenyl compounds mimicking all faces of the HIV-1 Rev protein positively-charged α-helix. Sci Rep 10:7190.

25. **Foster JL, Garcia JV.** 2008. HIV-1 Nef: At the crossroads. Retrovirology 5:84.

26. **González ME.** 2017. The HIV-1 Vpr protein: A multifaceted target for therapeutic intervention. Int J Mol Sci 18:126.

27. **González ME.** 2015. Vpu protein: The viroporin encoded by HIV-1. Viruses 7:4352–4368.

28. **Rose KM, Marin M, Kozak SL, Kabat D.** 2004. The viral infectivity factor (Vif) of HIV-1 unveiled. Trends Mol Med 10:291–297.

29. **Stopak K, de Noronha C, Yonemoto W, Greene WC.** 2003. HIV-1 Vif blocks the antiviral activity of APOBEC3G by impairing both its translation and intracellular stability. Mol Cell 12:591–601.

30. **Berthet-Colominas C, Monaco S, Novelli A, Sibaï G, Mallet F, Cusack S.** 1999. Head-to-tail dimers and interdomain flexibility revealed by the crystal structure of HIV-1 capsid protein (p24) complexed with a monoclonal antibody Fab. EMBO J 18:1124–1136.

31. **Campbell EM, Hope TJ.** 2015. HIV-1 capsid: the multifaceted key player in HIV-1 infection. Nature Reviews Microbiology;13(8):471–483.

32. **Barros M, Heinrich F, Datta SAK, Rein A, Karageorgos I, Nanda H, Lösche M.** 2016. Membrane binding of HIV-1 matrix protein: Dependence on bilayer composition and protein lipidation. J Virol 90:4544–4555.

33. **de la Arada I, Torralba J, Tascón I, Colom A, Ubarretxena-Belandia I, Arrondo JLR, Apellániz B, Nieva JL.** 2021. Conformational plasticity underlies membrane fusion induced by an HIV sequence juxtaposed to the lipid envelope. Sci Rep 11:1278.

34. **Dick RA, Mallery DL, Vogt VM, James LC.** 2018. IP6 regulation of HIV capsid assembly, stability, and uncoating. Viruses 10:640.

35. **Liu S, Harada BT, Miller JT, Le Grice SFJ, Zhuang X.** 2010. Initiation complex dynamics direct the transitions between distinct phases of early HIV reverse transcription. Nat Struct Mol Biol 17:1453–1460.

36. **Fassati A, Goff SP.** 2001. Characterization of intracellular reverse transcription complexes of human immunodeficiency virus type 1. J Virol 75:3626–3635.

37. **Dharan A, Bachmann N, Talley S, Zwikelmaier V, Campbell EM.** 2020. Nuclear pore blockade reveals that HIV-1 completes reverse transcription and uncoating in the nucleus. Nat Microbiol 5:1088–1095.

38. **Francis AC, Marin M, Prellberg MJ, Palermino-Rowland K, Melikyan GB.** 2020. HIV-1 uncoating and nuclear import precede the completion of reverse transcription in cell lines and in primary macrophages. Viruses 12:1234.

39. **Burdick RC, Delviks-Frankenberry KA, Chen J, Janaka SK, Sastri J, Hu W-S, Pathak VK.** 2017. Dynamics and regulation of nuclear import and nuclear movements of HIV-1 complexes. PLoS Pathog 13:e1006570.

40. **Delelis O, Carayon K, Saïb A, Deprez E, Mouscadet J-F.** 2008. Integrase and integration: biochemical activities of HIV-1 integrase. Retrovirology 5:114.

41. **Francis AC, Melikyan GB.** 2018. Single HIV-1 imaging reveals progression of infection through CA-dependent steps of docking at the nuclear pore, uncoating, and nuclear transport. Cell Host Microbe 23:536-548.e6.

42. **Toccafondi E, Lener D, Negroni M.** 2021. HIV-1 capsid core: A bullet to the heart of the target cell. Front Microbiol 12:652486.

43. **Burdick RC, Li C, Munshi M, Rawson JMO, Nagashima K, Hu W-S, Pathak VK.** 2020. HIV-1 uncoats in the nucleus near sites of integration. Proc Natl Acad Sci U S A 117:5486–5493.

44. **Hulme AE, Kelley Z, Foley D, Hope TJ.** 2015. Complementary assays reveal a low level of CA associated with viral complexes in the nuclei of HIV-1-infected cells. J Virol 89:5350–5361.

45. **Di Nunzio F, Danckaert A, Fricke T, Perez P, Fernandez J, Perret E, Roux P, Shorte S, Charneau P, Diaz-Griffero F, Arhel NJ.** 2012. Human nucleoporins promote HIV-1 docking at the nuclear pore, nuclear import and integration. PLoS One 7:e46037.

46. **Dharan A, Talley S, Tripathi A, Mamede JI, Majetschak M, Hope TJ, Campbell EM.** 2016. KIF5B and Nup358 cooperatively mediate the nuclear import of HIV-1 during infection. PLoS Pathog 12:e1005700.

47. **Elliott JL, Kutluay SB.** 2020. Going beyond integration: The emerging role of HIV-1 integrase in virion morphogenesis. Viruses 12:1005.

48. HIV/AIDS. https://www.niaid.nih.gov/diseases-conditions/hivaids. Retrieved 6 December 2021.

49. **Santa-Marta M, de Brito PM, Godinho-Santos A, Goncalves J.** 2013. Host factors and HIV-1 replication: Clinical evidence and potential therapeutic approaches. Front Immunol 4:343.

50. **Wang L, Zhang H, Solski PA, Hart MJ, Der CJ, Su L.** 2000. Modulation of HIV-1 replication by a novel RhoA effector activity. J Immunol 164:5369–5374.

51. **Carnes SK, Zhou J, Aiken C.** 2018. HIV-1 engages a dynein-dynactin-BICD2 complex for infection and transport to the nucleus. J Virol 92:JVI.00358-18.

52. **Lukic Z, Dharan A, Fricke T, Diaz-Griffero F, Campbell EM.** 2014. HIV-1 uncoating is facilitated by dynein and kinesin 1. J Virol 88:13613–13625.

53. **Fernandez J, Portilho DM, Danckaert A, Munier S, Becker A, Roux P, Zambo A, Shorte S, Jacob Y, Vidalain P-O, Charneau P, Clavel F, Arhel NJ.** 2015. Microtubule-associated proteins 1 (MAP1) promote human immunodeficiency virus type I (HIV-1) intracytoplasmic routing to the nucleus. J Biol Chem 290:4631–4646.

54. **McDonald D, Vodicka MA, Lucero G, Svitkina TM, Borisy GG, Emerman M, Hope TJ.** 2002. Visualization of the intracellular behavior of HIV in living cells. J Cell Biol 159:441–452.

55. **Fletcher DA, Mullins RD.** 2010. Cell mechanics and the cytoskeleton. Nature 463:485–492.

56. **Dai L, Lidie KB, Chen Q, Adelsberger JW, Zheng X, Huang D, Yang J, Lempicki RA, Rehman T, Dewar RL, Wang Y, Hornung RL, Canizales KA, Lockett SJ, Lane HC, Imamichi T.** 2013. IL-27 inhibits HIV-1 infection in human macrophages by down-regulating host factor SPTBN1 during monocyte to macrophage differentiation. J Exp Med 210:517–534.

57. **Berk A, Kaiser CA, Lodish H, Amon A, Ploegh H, Bretscher A, Krieger M, Martin KC.** 2016. Molecular Cell Biology, 8th ed. W.H. Freeman, New York, NY.

58. **Jolly C, Mitar I, Sattentau QJ.** 2007. Requirement for an intact T-cell actin and tubulin cytoskeleton for efficient assembly and spread of human immunodeficiency virus type 1. J Virol 81:5547–5560.

59. **Yoder A, Yu D, Dong L, Iyer SR, Xu X, Kelly J, Liu J, Wang W, Vorster PJ, Agulto L, Stephany DA, Cooper JN, Marsh JW, Wu Y.** 2008. HIV envelope-CXCR4 signaling activates cofilin to overcome cortical actin restriction in resting CD4 T cells. Cell 134:782–792.

60. **Spear M, Guo J, Wu Y.** 2012. The trinity of the cortical actin in the initiation of HIV-1 infection. Retrovirology 9:45.

61. **Gallo SA, Puri A, Blumenthal R.** 2001. HIV-1 gp41 six-helix bundle formation occurs rapidly after the engagement of gp120 by CXCR4 in the HIV-1 Env-mediated fusion process. Biochemistry 40:12231–12236.

62. **Jolly C, Kashefi K, Hollinshead M, Sattentau QJ.** 2004. HIV-1 cell to cell transfer across an Env-induced, actin-dependent synapse. J Exp Med 199:283–293.

63. **Gladnikoff M, Shimoni E, Gov NS, Rousso I.** 2009. Retroviral assembly and budding occur through an actin-driven mechanism. Biophys J 97:2419–2428.

64. **Sasaki H, Nakamura M, Ohno T, Matsuda Y, Yuda Y, Nonomura Y.** 1995. Myosin-actin interaction plays an important role in human immunodeficiency virus type 1 release from host cells. Proc Natl Acad Sci U S A 92:2026–2030.

65. **Arhel N, Genovesio A, Kim K-A, Miko S, Perret E, Olivo-Marin J-C, Shorte S, Charneau P.** 2006. Quantitative four-dimensional tracking of cytoplasmic and nuclear HIV-1 complexes. Nat Methods 3:817–824.

66. **Iyengar S, Hildreth JEK, Schwartz DH.** 1998. Dependent Receptor Colocalization Required for Human Immunodeficiency Virus Entry into Host Cells. Journal of Virology 72:5251–5255.

67. **Jiménez-Baranda S, Gómez-Moutón C, Rojas A, Martínez-Prats L, Mira E, Ana Lacalle R, Valencia A, Dimitrov DS, Viola A, Delgado R, Martínez-A C, Mañes S.** 2007. Filamin-A regulates actin-dependent clustering of HIV receptors. Nat Cell Biol 9:838–846.

68. **Brass AL, Dykxhoorn DM, Benita Y, Yan N, Engelman A, Xavier RJ, Lieberman J, Elledge SJ.** 2008. Identification of host proteins required for HIV infection through a functional genomic screen. Science 319:921–926.

69. **Hayes NVL, Scott C, Heerkens E, Ohanian V, Maggs AM, Pinder JC, Kordeli E, Baines AJ.** 2000. Identification of a novel C-terminal variant of beta-II spectrin: two isoforms of beta-II spectrin have distinct intracellular locations and activities. J Cell Sci 113:2023–2034.

70. **Yang P, Yang Y, Sun P, Tian Y, Gao F, Wang C, Zong T, Li M, Zhang Y, Yu T, Jiang Z.** 2021. βII spectrin (SPTBN1): biological function and clinical potential in cancer and other diseases. Int J Biol Sci 17:32–49.

71. **Brown JW, Bullitt E, Sriswasdi S, Harper S, Speicher DW, McKnight CJ.** 2015. The physiological molecular shape of spectrin: A compact supercoil resembling a Chinese Finger Trap. PLoS Comput Biol 11:e1004302.

72. **Scoles DR, Huynh DP, Morcos PA, Coulsell ER, Robinson NG, Tamanoi F, Pulst SM.** 1998. Neurofibromatosis 2 tumour suppressor schwannomin interacts with betaII-spectrin. Nat Genet 18:354–359.

73. **Miyauchi K, Kim Y, Latinovic O, Morozov V, Melikyan GB.** 2009. HIV enters cells via endocytosis and dynamin-dependent fusion with endosomes. Cell 137:433–444.

74. **Gallo DE, Hope TJ.** 2012. Knockdown of MAP4 and DNAL1 produces a post-fusion and pre-nuclear translocation impairment in HIV-1 replication. Virology 422:13–21.

75. **Havlicek MG.** 2022. The role of the host factor SPTBN1 in HIV-1 infection of microglial cells. Missouri State University.

76. **Janabi N, Peudenier S, Héron B, Ng KH, Tardieu M.** 1995. Establishment of human microglial cell lines after transfection of primary cultures of embryonic microglial cells with the SV40 large T antigen. Neurosci Lett 195:105–108.

77. Standard transformation protocol for multiple-use cells E. coli competent cells: Multiple-use protocol. https://www.promega.com/-/media/files/resources/protcards/e-coli-competent-cells-quick-protocol.pdf?rev=81255b2b910545eb8c4c176dc722b7cf&sc_lang=en. Retrieved 9 November 2022.

78. 2021. Qiagen Plasmid Purification Handbook. qiagen.com. https://www.qiagen.com/us/resources/download.aspx?id=0bd0c5fb-c271-43e7-af43-32d539374fa9&lang=en. Retrieved 9 November 2022.

79. **Fuentes M.** 2013. Hemocytometer protocol •. Hemocytometer. https://www.hemocytometer.org/hemocytometer-protocol/. Retrieved 10 November 2022.

80. 2013. RNAiMAX Transfection Protocol. Thermofisher.com. https://www.thermofisher.com/document-connect/document-

connect.html?url=https://assets.thermofisher.com/TFS-Assets/LSG/manuals/Lipofectamine_RNAiMAX_Reag_protocol.pdf. Retrieved 9 November 2022.

81. SsoFast EvaGreen Supermix. Bio-Rad.com. https://www.bio-rad.com/webroot/web/pdf/lsr/literature/10014647A.pdf. Retrieved 9 November 2022.

82. iTaq Universal Probes One-Step Kit. Bio-Rad.com. https://www.bio-rad.com/webroot/web/pdf/lsr/literature/10032046.pdf. Retrieved 9 November 2022.

83. **Gallagher SR, Wiley EA.** 2012. Current Protocols Essential Labratory Techniques. Wiley.

84. **Ingram Z, Taylor M, Okland G, Martin R, Hulme AE.** 2020. Characterization of HIV-1 uncoating in human microglial cell lines. Virol J 17:31.

85. **Hulme AE, Kelley Z, Okocha EA, Hope TJ.** 2015. Identification of capsid mutations that alter the rate of HIV-1 uncoating in infected cells. J Virol 89:643–651.

86. **Van Holm W, Ghesquière J, Boon N, Verspecht T, Bernaerts K, Zayed N, Chatzigiannidou I, Teughels W.** 2021. A viability quantitative PCR dilemma: Are longer amplicons better? Appl Environ Microbiol 87:e0265320.

87. iTaq DNA Polymerase. Bio-rad.com. https://www.bio-rad.com/webroot/web/pdf/lsr/literature/4106202B.pdf. Retrieved 17 October 2022.

88. SsoFast EvaGreen supermixes. Bio-Rad Laboratories. https://www.bio-rad.com/en-us/product/ssofast-evagreen-supermixes?ID=MH5HL6MNI. Retrieved 3 October 2022.

89. Real-Time PCR and qPCR Supermixes Selection Guide. Bio-Rad.com. https://www.bio-rad.com/webroot/web/html/lsr/products/amplification_pcr/category_overlay/global/supermixes_selection_guide.html. Retrieved 3 October 2022.

90. **Duxbury MS, Ashley SW, Whang EE.** 2005. RNA interference: a mammalian SID-1 homologue enhances siRNA uptake and gene silencing efficacy in human cells. Biochem Biophys Res Commun 331:459–463.

91. **Li Q, Barres BA.** 2018. Microglia and macrophages in brain homeostasis and disease. Nat Rev Immunol 18:225–242.

92. **Aggarwal A, Hitchen TL, Ootes L, McAllery S, Wong A, Nguyen K, McCluskey A, Robinson PJ, Turville SG.** 2017. HIV infection is influenced by dynamin at 3 independent points in the viral life cycle. Traffic 18:392–410.

93. **Casella CR, Raffini LJ, Panganiban AT.** 1997. Pleiotropic mutations in the HIV-1 matrix protein that affect diverse steps in replication. Virology 228:294–306.

94. **Reicin AS, Ohagen A, Yin L, Hoglund S, Goff SP.** 1996. The role of Gag in human immunodeficiency virus type 1 virion morphogenesis and early steps of the viral life cycle. J Virol 70:8645–8652.

95. **Bukrinskaya A, Brichacek B, Mann A, Stevenson M.** 1998. Establishment of a functional human immunodeficiency virus type 1 (HIV-1) reverse transcription complex involves the cytoskeleton. J Exp Med 188:2113–2125.

APPENDIX: RESEARCH COMPLIANCE CERTIFICATIONS

July 18, 2022

RE: IBC protocols 2022-02.3 & 2022-02.4

Dear Graduate College,

Protocols #2022-02.3 & 2022-02.4 entitled "Studies on the early steps of HIV-1 replication" for biohazards and rDNA, are Institutional Biosafety Committee (IBC) reviewed protocols originating from 2016. These protocols have been consistently updated per IBC policy since 2016. The latest approvals were dated 2/24/2022 to 2/23/2024, submitted by Dr. Amy Hulme, Ph.D.

Thank you and if you need anything in the future regarding these protocols, please contact me via email (johnnapedersen@missouristate.edu) or at 417-836-3737.

Sincerely,

Johnna Pedersen

Missouri State
UNIVERSITY

October 8, 2022

RE: IBC protocols 2022-02.3 & 2022-02.4

Hello Hannah Matheney,

IBC protocols #2022-02.3 & 2022-02.4 entitled "Studies on the early steps of HIV-1 replication" for biohazards and rDNA, were continued projects and approved 2/24/2022 to 2/23/2024. You are an approved member to work with Dr. Amy Hulme, Ph.D. on these protocols.

Thank you and if you need anything in the future regarding these protocols, please contact me via email (johnnapedersen@missouristate.edu) or at 417-836-3737.

Sincerely,

Johnna Pedersen

Johnna Pedersen

CITI PROGRAM

Completion Date 04-Feb-2022
Expiration Date 04-Feb-2024
Record ID 46790333

This is to certify that:

Hannah Matheney

Has completed the following CITI Program course:

Not valid for renewal of certification through CME.

Biosafety and Biosecurity (BSS)
(Curriculum Group)
Basic Biosafety Course
(Course Learner Group)
1 - Basic Course
(Stage)

Under requirements set by:

Missouri State University

CITI
Collaborative Institutional Training Initiative

Verify at www.citiprogram.org/verify/?w4097a703-b437-45b5-b6c6-537ac9cf24c5-46790333

CITI PROGRAM

Completion Date 27-Mar-2019
Expiration Date 26-Mar-2021
Record ID 31080423

This is to certify that:

Hannah Matheney

Has completed the following CITI Program course:

Not valid for renewal of certification through CME.

Biosafety and Biosecurity (BSS)
(Curriculum Group)
Basic Biosafety Course
(Course Learner Group)
1 - Basic Course
(Stage)

Under requirements set by:

Missouri State University

CITI
Collaborative Institutional Training Initiative

Verify at www.citiprogram.org/verify/?w4cc4856e-6dc4-4a09-bf61-bb0d3da541d3-31080423